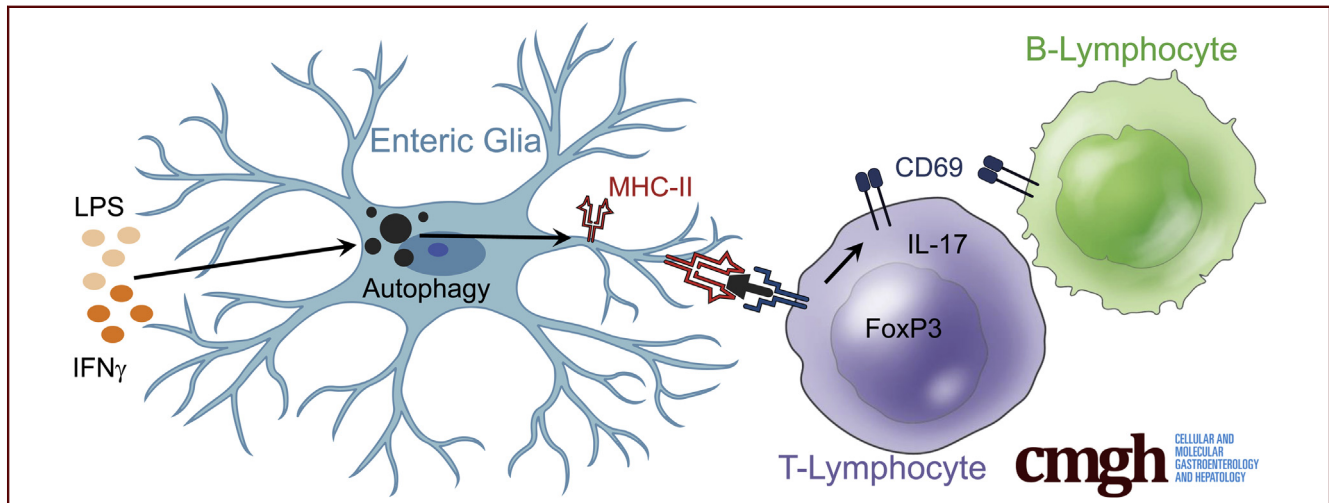


ORIGINAL RESEARCH

Enteric Glia Regulate Lymphocyte Activation via Autophagy-Mediated MHC-II Expression

Aaron K. Chow,¹ Vladimir Grubišić,¹ and Brian D. Gulbransen^{1,2}¹Department of Physiology, ²Neuroscience Program, Michigan State University, East Lansing, Michigan

SUMMARY

Enteric glia express major histocompatibility group class II antigens in response to the proinflammatory stimuli interferon- γ and lipopolysaccharide. Glial major histocompatibility group class II expression requires autophagy pathways and functions to regulate B- and T-lymphocyte activation, with specific effects on T-lymphocyte subsets involved in tolerance.

BACKGROUND & AIMS: Enteric glial cells express type II major histocompatibility complex (MHC-II) molecules in Crohn's disease and Chagas disease, but it is unclear whether the expressed molecules are functional. We examined the capabilities of enteric glia to act as an antigen-presenting cell in vivo and whether glial MHC-II has immunomodulatory effects.

METHODS: We generated *Sox10^{CreERT2};IAB^{f/f}* mice to ablate MHC-II in enteric glia after exposure to tamoxifen. We measured phagocytic activity and autophagy activation to assess potential peptide sources loaded onto glial MHC-II and measured T- and B-lymphocyte activation and serum and colonic tissue cytokine levels to study enteric glial immunomodulatory capabilities.

RESULTS: Enteric glia express MHC-II molecules in response to a subclinical dose of interferon- γ and lipopolysaccharide in vivo. Glial MHC-II expression contributes to effective B-lymphocyte and T-lymphocyte activation with marked effects on T-helper cell (Th)17 and regulatory T cell subtypes. No

effect on Th1 or Th2 subtypes was observed. Enteric glial MHC-II does not have a major effect on serum or colonic tissue cytokine levels but may influence local cytokine levels. Glial MHC-II expression requires the activation of autophagy pathways, but activating autophagy alone is not sufficient to drive glial MHC-II expression.

CONCLUSIONS: Enteric glia express MHC-II as a mechanism to tune intestinal immune responses. Glial autophagy is triggered in response to proinflammatory stimuli and induces glial antigen presentation, which functions to modulate the activation of T-lymphocyte subsets involved in tolerance. These observations suggest that enteric glia may express MHC-II to maintain immune homeostasis during inflammatory conditions such as Crohn's disease. (*Cell Mol Gastroenterol Hepatol* 2021;12:1215-1237; <https://doi.org/10.1016/j.jcmgh.2021.06.008>)

Keywords: Enteric Glial Cell; Autophagy; Major Histocompatibility Complex Type II; T-Lymphocyte.

Antigen presentation is a crucial process that maintains immune homeostasis by dictating T-lymphocyte activation at the transition between the innate and adaptive arms of the immune system. Dysfunction in antigen presentation can lead to the underactivation or overactivation of the immune system, or immune activation against inappropriate targets.¹ As a consequence, presenting the correct antigens and directing immune activity against the proper targets is of prime importance in the gastrointestinal tract, where bacteria, viruses, parasites, and other

foreign particles are constant challenges. Dysfunction in antigen presentation is a major contributing factor to immune dysregulation in diseases such as systemic lupus erythematosus, multiple sclerosis, and inflammatory bowel disease.¹

Professional antigen-presenting cells are the primary cell types responsible for the process of antigen presentation and use major histocompatibility complex type II (MHC-II) molecules to present specific peptides to T-lymphocytes. However, in addition to professional antigen-presenting cells expressing MHC-II molecules, a set of atypical MHC-II-expressing cells, such as endothelial cells, epithelial cells, mast cells, and glial cells, show variable levels of MHC-II expression.^{2,3} Among these, enteric glia have gained considerable interest based on their ability to affect both T-lymphocyte activation and neuronal signaling.^{4,5} Enteric glial cells express MHC-II molecules in an inducible manner, and share similar characteristics with antigen-presenting cells by expressing T-lymphocyte costimulatory molecules CD80 and CD86.^{6–8} Enteric glia are capable of expressing proinflammatory and anti-inflammatory cytokines, and can interact with T-lymphocytes and modulate their activation *in vitro*.^{4,9} Although glial-T-lymphocyte interactions have been alluded to by *in vitro* studies, whether enteric glia play a significant role as antigen-presenting cells *in vivo* is not known.

The goal of this study was to test the hypothesis that glial antigen presentation modulates immune homeostasis in the intestine through interactions with CD4+ T-lymphocytes. We tested our hypothesis using a subclinical proinflammatory stimulus composed of interferon- γ (IFN γ) and lipopolysaccharide (LPS) to perturb immune homeostasis without driving overt inflammation, and tested the role of glial MHC-II by generating mice with a conditional ablation of MHC-II in enteric glia. The data show that enteric glia express MHC-II in response to IFN γ and LPS and that glial MHC-II expression is necessary for adequate CD4+ and CD8+ T-lymphocyte activation, and CD19+ B-lymphocyte activation. Ablating glial antigen presentation impaired the activation of T-lymphocyte subsets expressing interleukin (IL)17 and forkhead box protein P3 (FoxP3), suggesting that glial antigen presentation influences T helper cell (Th)17 and regulatory T cell (T_{reg}) activation. Glial antigen presentation was independent of an increase in phagocytic activity and required the activation of autophagy. Taken together, these results show that glial autophagy triggered in response to proinflammatory stimuli induces glial antigen presentation, which functions to modulate the activation of T-lymphocyte subsets involved in tolerance.

Results

Conditional Ablation of Glial MHC-II in *Glial*^{Major} histocompatibility complex type II knockout (*MHC2KO*) Mice and IFN γ + LPS Challenge

Enteric glia express MHC-II in response to proinflammatory stimuli such as LPS and IFN γ (Figure 1A, D–F).⁷ These stimuli also elicit antigen presentation by professional immune cells, which can mask the contribution of glia. Therefore, we used a minimal proinflammatory stimulus (1 μ g IFN γ /mouse, 0.3 mg/kg LPS; both administered

intraperitoneally) to study glial effects *in vivo* without an overwhelming inflammatory response from other immune cells (Figure 1C). This subclinical challenge is sufficient to induce glial MHC-II (Figure 1D–F) and causes minor weight loss (Figure 2A), but does not increase sickness behavior (Figure 2B), alter tissue architecture (Figure 2D), cause significant histologic damage (Figure 2C), induce changes in glial fibrillary acidic protein (GFAP) expression in enteric glia (Figure 2E), or induce changes in enteric neuronal density in the myenteric plexus (Figure 2F).

Murine MHC-II molecules are composed of gene products from the I-A or I-E loci. C57BL/6 mice have a deficient I-E loci and rely solely on the I-A loci for MHC-II expression.¹⁰ *Glial*^{Major} Histocompatibility Complex Type II Knockout (*MHC2KO*) mice with a glial-specific inducible MHC-II deletion (*Sox10*^{CreERT2}; *IAB*^{f/f}) were used to isolate the specific role of enteric glial MHC-II expression (Figure 1B and C).

Enteric Glia Express Mature MHC-II in Response to IFN γ + LPS

Enteric glia increased MHC-II expression in animals challenged with IFN γ and LPS despite no overt inflammation tissue architecture changes, or indications of reactive gliosis or neuronal damage (Figures 1D and 2). Within enteric ganglia, MHC-II expression is limited to glia and no neuronal expression was observed (Figure 1D). Confocal image analyses confirm that MHC-II primarily colocalizes with GFAP-labeled enteric glia in enteric ganglia (Mander's overlap coefficient, 90%) (Figure 1E and F). Control animals treated with IFN γ and saline did not show glial MHC-II expression (Figure 1D). Quantification of MHC-II immunolabeling shows that enteric glia significantly ($P = .0370$) up-regulate MHC-II expression in response to IFN γ and LPS in wild-type animals, and that this effect is absent in *glial*^{MHC2KO} animals (Figure 1G). Muscularis macrophages at the level of the myenteric plexus show constitutive expression of MHC-II,¹¹ and exposure to IFN γ and LPS stimuli did not alter expression level or pattern in wild-type or *glial*^{MHC2KO} animals (Figure 3A and B). These observations are consistent with prior data showing that LPS stimulates enteric glial MHC-II expression through Toll-like receptor 4 (TLR4) pathways^{7,9} and that enteric neurons lack expression of TLR4 and MHC-II.¹² Importantly, these results show that the *glial*^{MHC2KO} mouse model effectively ablates MHC-II expression specifically in enteric glia and not within immune cells, thereby isolating any changes in immune activation to enteric glia.

Abbreviations used in this paper: 3-MA, 3-methyladenine; ANOVA, analysis of variance; ENS, enteric nervous system; FoxP3, Forkhead box protein P3; GFAP, glial fibrillary acidic protein; IAB, histocompatibility 2, class II antigen A, beta 1; IFN γ , interferon- γ ; IL, interleukin; LPS, lipopolysaccharide; MHC-II, major histocompatibility complex II; PBS, phosphate-buffered saline; Th, T helper cell; Treg, regulatory T cell.

 Most current article

© 2021 The Authors. Published by Elsevier Inc. on behalf of the AGA Institute. This is an open access article under the CC BY-NC-ND license (<http://creativecommons.org/licenses/by-nc-nd/4.0/>).

2352-345X

<https://doi.org/10.1016/j.jcmgh.2021.06.008>

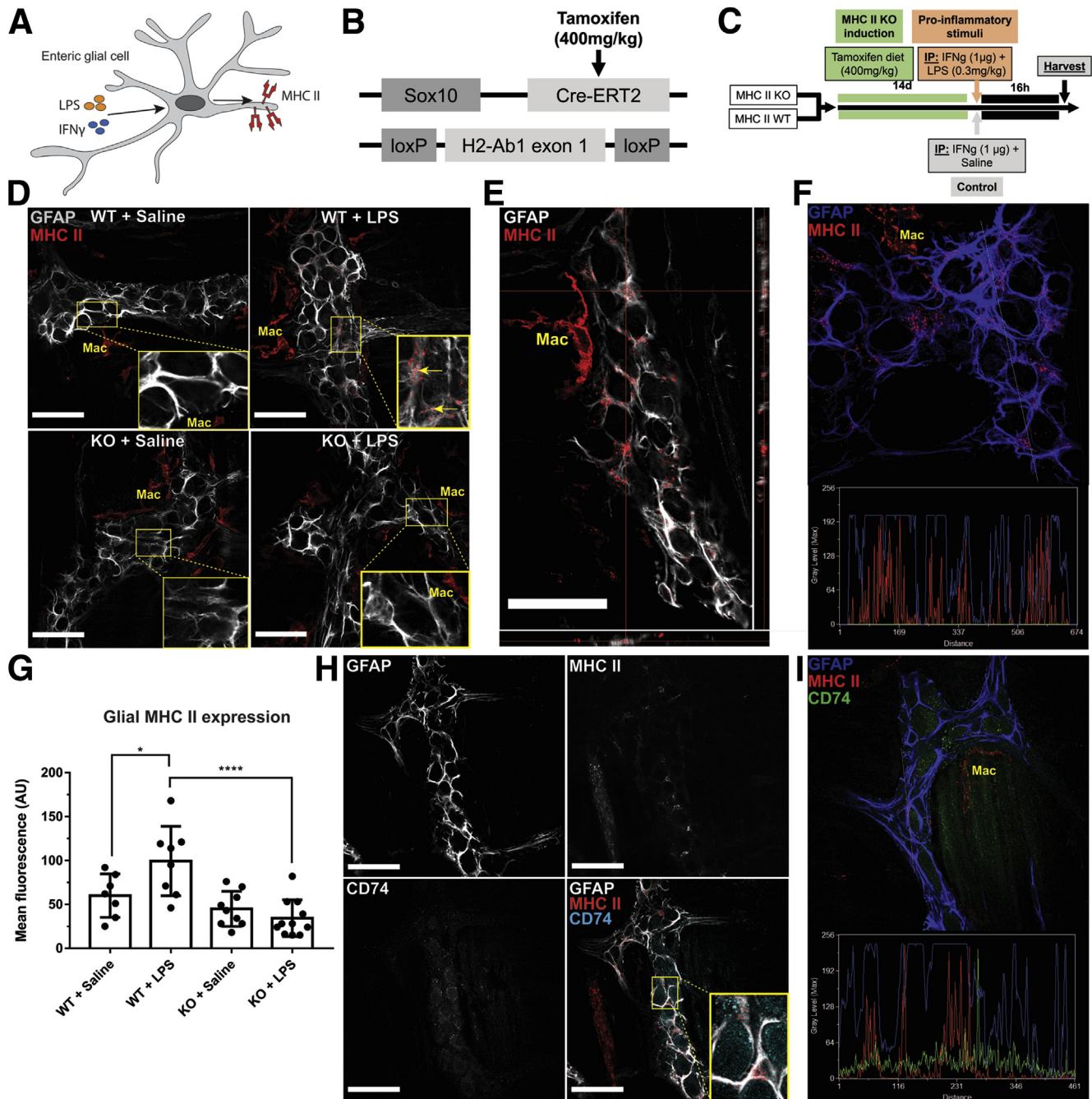


Figure 1. Enteric glial cells express MHC-II when stimulated with IFN γ and LPS. (A) Schematic showing enteric glial cells expressing MHC-II molecules as a response to exposure to 1 μ g IFN γ and 0.3 mg/kg LPS. (B) Schematic showing the gene-targeting strategy in *Sox10^{CreERT2}; IAB^{fl/fl}* (glial^{MHC2KO}) mice. Tamoxifen-sensitive Cre^{ERT2} expression is confined to glia by the *Sox10* promoter and excises the floxed *H2-Ab1* exon 1 loci. (C) Schematic showing the proinflammatory exposure protocol. (D) Representative confocal images of GFAP (grey) and MHC-II (red) immunofluorescence labeling in enteric ganglia of glial^{MHC2KO} (knockout [KO]) vs wild-type littermates when pretreated with IFN γ and then challenged with LPS or saline control. Enteric glia express MHC-II when stimulated with IFN γ and LPS. Muscularis macrophages (Mac) bordering enteric ganglia show constitutive MHC-II expression in all conditions. (E) Orthogonal views of confocal z-stacks show MHC-II (red) labeling in GFAP-expressing (grey) enteric glia. (F) Line-scans through enteric ganglia show co-expression of MHC-II (red) and GFAP (blue) labeling. (G) Quantified mean fluorescent intensity of MHC-II labeling on GFAP-expressing enteric glia in the myenteric plexus (n = 7–11 mice). Two-way analysis of variance with Tukey-corrected multiple comparisons; **P* < .05, *****P* < .0001. (H) Representative confocal images of GFAP (grey), MHC-II (red), and CD74 (cyan) immunolabeling in wild-type animals treated with IFN γ and LPS show a neuronal and glial distribution of CD74. (I) Line-scans through enteric ganglia show minimal overlap between MHC-II (red) and CD74 (green) in GFAP-expressing (blue) enteric glia. Scale bars: 50 μ m. IP, intraperitoneally.

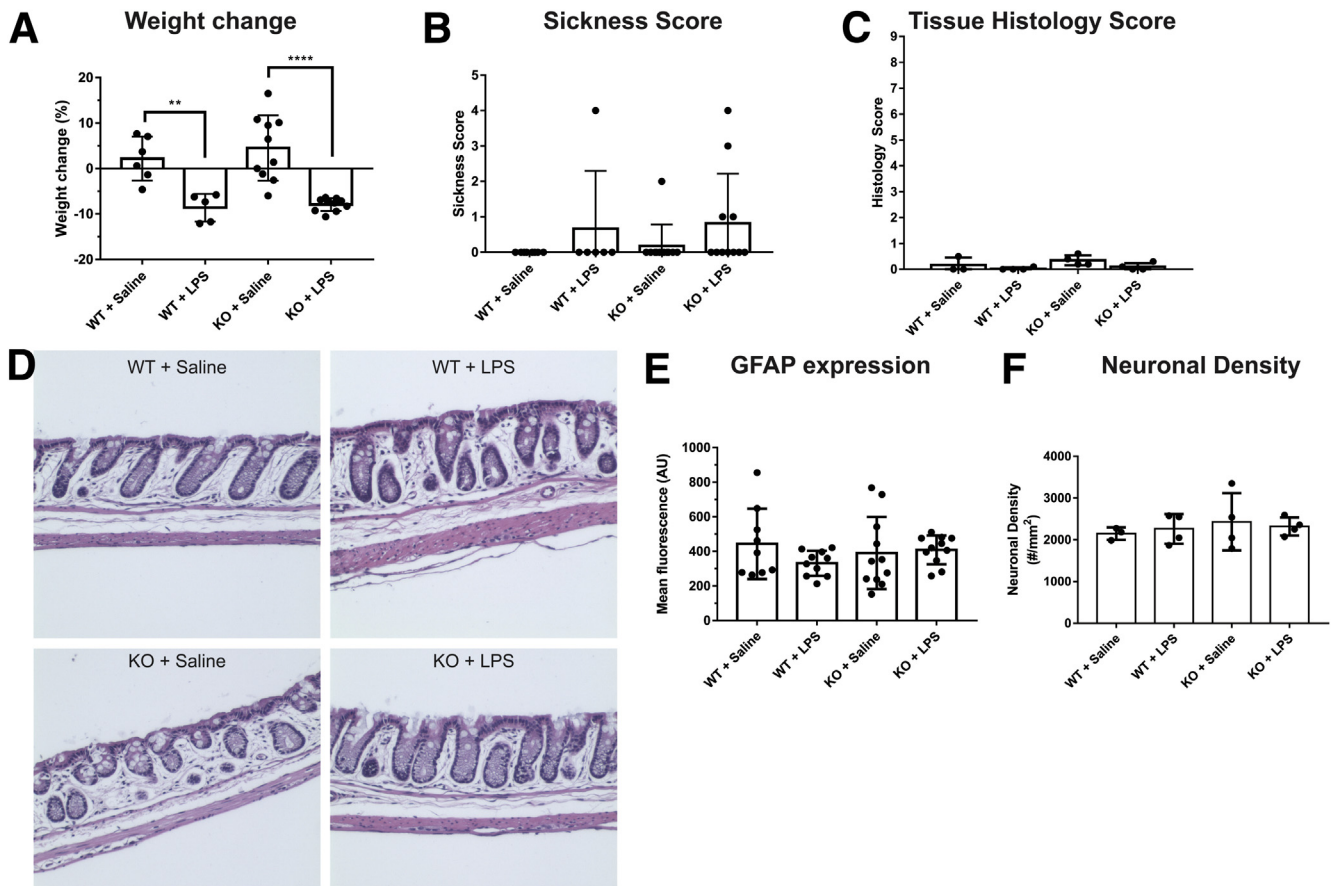


Figure 2. Exposure to IFN γ and LPS causes weight loss but does not cause significant tissue damage or observable inflammation. Animals treated with IFN γ + LPS show (A) weight loss (wild-type, ** $P = .0054$; knockout [KO], **** $P < .0001$; $n = 5-10$ mice; 2-way analysis of variance with Tukey-corrected multiple comparisons) but do not show (B) significant sickness, (C) increased tissue histology scores, (D) changes in colonic tissue architecture, (E) changes in glial GFAP expression, or (F) myenteric neuron density.

In antigen-presenting cells, immature MHC-II molecules contain CD74 bound within their peptide-binding groove until fusion with phagolysosomes when the CD74 dissociates to allow loading of processed peptides.¹³ We tested whether the MHC-II molecules expressed by enteric glia are mature by labeling for CD74. CD74 immunoreactivity was present in both enteric neurons and glia (Figure 1H), and this is consistent with the pattern of *Cd74* gene expression in enteric neurons and glia.¹² However, no co-labeling of enteric glial MHC-II and CD74 was detected (Figure 1H). Furthermore, line-scans through enteric ganglia show little colocalization between CD74 and MHC-II (Mander's overlap coefficient, 2%) (Figure 1I). Together, these results show that enteric glia are sensitive to proinflammatory stimuli and respond to low doses of IFN γ and LPS by expressing mature MHC-II molecules.

Enteric Glia-Specific MHC-II Signaling Significantly Contributes to the Activation of Immune Cells in the Mesenteric Lymph Node

Because the MHC-II signaling pathway is one of the essential lines of communication between innate and

adaptive immune cells, we hypothesized that the IFN γ /LPS-induced MHC-II expression on enteric glia will significantly affect lymphocyte activation. We treated glial^{MHC2KO} mice and their wild-type littermate controls with either IFN γ + saline or IFN γ + LPS and used flow cytometry to quantify cells expressing CD69, an early stage activation marker, in the gut-draining mesenteric lymph nodes and the skin-draining inguinal lymph nodes (Figure 4). Although LPS treatment induced a comparable increase in the CD69+ cells in mesenteric and inguinal lymph nodes (means \pm SD, 71% \pm 8% and 70% \pm 20%, respectively), ablating glial MHC-II in glial^{MHC2KO} animals significantly blunted immune cell activation in mesenteric lymph nodes but had no significant effect on the CD69+ cell population in inguinal lymph nodes ($P = .022$ and .424, 2-way analysis of variance [ANOVA] with Sidak's adjusted multiple comparisons) (Figure 4C). These results show that the main effect of enteric glial MHC-II is specific for the gut-draining lymph nodes and suggest a direct interaction between enteric glia and immunocytes residing in the gut wall.

We then phenotyped the cells and observed that on average at least 95% of CD69+ cells from the LPS-treated lymph nodes are either CD19+ or CD3+ (Figure 5),

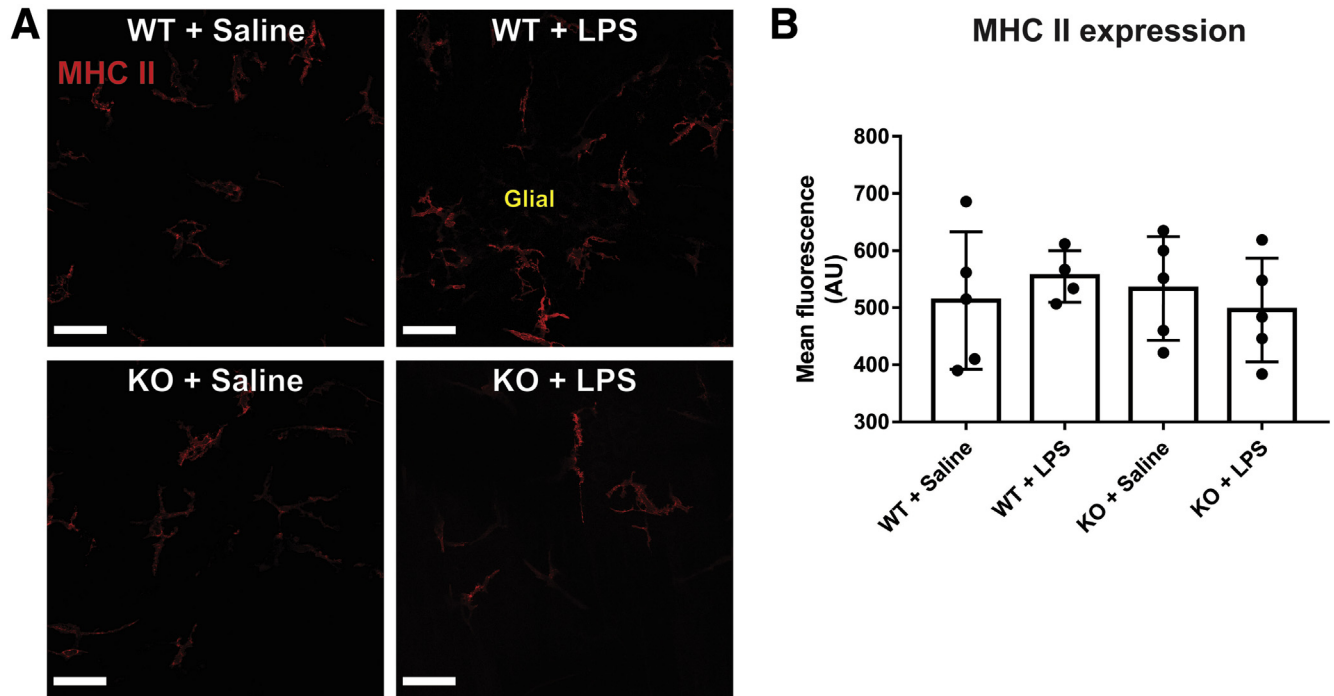


Figure 3. Macrophage MHC II expression is not altered by IFN γ and LPS. (A) Representative confocal images of MHC II (red) immunofluorescent labeling in enteric ganglion. Scale bars: 50 μ m. (B) Quantified mean fluorescent intensity of MHC II labeling in muscularis macrophages bordering enteric ganglion ($n = 4$ –5 mice; 2-way analysis of variance with Tukey-corrected multiple comparisons). KO, knockout.

markers of B and T-lymphocytes. The proportions of the double-positive CD69+/CD19+ and CD69+/CD3+ cells were comparable between the LPS-treated glial^{MHC2KO} animals and their wild-type littermates ($P > .12$, 2-way ANOVA with Sidak's adjusted multiple comparisons) (Figure 5B). Together, these findings indicate that in the lymph nodes LPS exclusively activates lymphocytes, comparably B and T cells, and ablating glial MHC-II does not affect the proportion of the activated lymphocytes.

Enteric Glial MHC-II Expression Contributes to CD4+ and CD8+ T-Lymphocyte Activation

MHC-II molecules expressed by professional antigen-presenting cells play an important role in interactions that activate T-lymphocytes and our findings indicate a possible direct interplay between the enteric glial MHC-II and activation of resident lymphocytes (Figure 4C). Therefore, we tested whether glial MHC-II molecules are functionally relevant in antigen presentation to T-lymphocytes. We began by using immunolabeling to examine whether enteric glia and T-lymphocytes are within sufficient proximity for potential interactions. In support, CD4+ T-lymphocytes were observed within 2 μ m of GFAP+ enteric glia at the level of the myenteric plexus, consistent with recent reports showing that T-lymphocytes preferentially associate with neurons and glia in the myenteric plexus (Figure 6B).¹⁴ Next, we tested whether glial MHC-II mediates functional interactions with T-lymphocytes that influence their activation state by measuring CD69 expression in wild-type control and glial^{MHC2KO} animals.

The majority of CD4+ cells are in an inactive state in wild-type control animals treated with IFN γ + saline, and only 38% \pm 8% of CD4+ cells expressed the acute activation marker CD69 (Figure 6C and D). Exposure to IFN γ and LPS expanded the population of activated CD4+ cells by 29% and increased the percentage of CD4+ cells expressing CD69 to 67% \pm 13% ($P = .0010$). Ablating glial MHC-II significantly ($P = .0309$) blunted the effect of IFN γ and LPS and decreased the proportion of CD4+ cells expressing CD69 to 46% \pm 17%, which is similar to the proportion of active CD4+ cells observed in control animals treated with IFN γ + saline (Figure 6D). Glial MHC-II ablation had no effect on the percentage of activated CD4+ cells in IFN γ + saline-treated control animals (38% \pm 19%) (Figure 6C and D), and this is expected given that glial MHC-II expression is observed only in animals challenged with LPS (Figure 1). Enteric glial MHC-II expression also affected CD8+ T-lymphocyte activation in mesenteric lymph nodes (Figure 6E and F). In healthy wild-type control animals treated with IFN γ + saline, 61% \pm 6% of CD8+ T-lymphocytes expressed CD69, and this proportion increased significantly to 87% \pm 4% in wild-type animals challenged with IFN γ and LPS ($P = .0132$) (Figure 6F). However, the IFN γ and LPS challenge did not affect CD8+ T-lymphocyte activation in glial^{MHC2KO} animals (Figure 6F). Together, these results show that enteric glial antigen presentation mediated by MHC-II plays an important role in regulating immune activity through effects on CD4+ and CD8+ T-lymphocytes.

Because enteric glial MHC-II ablation influences the activation state of CD4+ T-lymphocytes, we examined

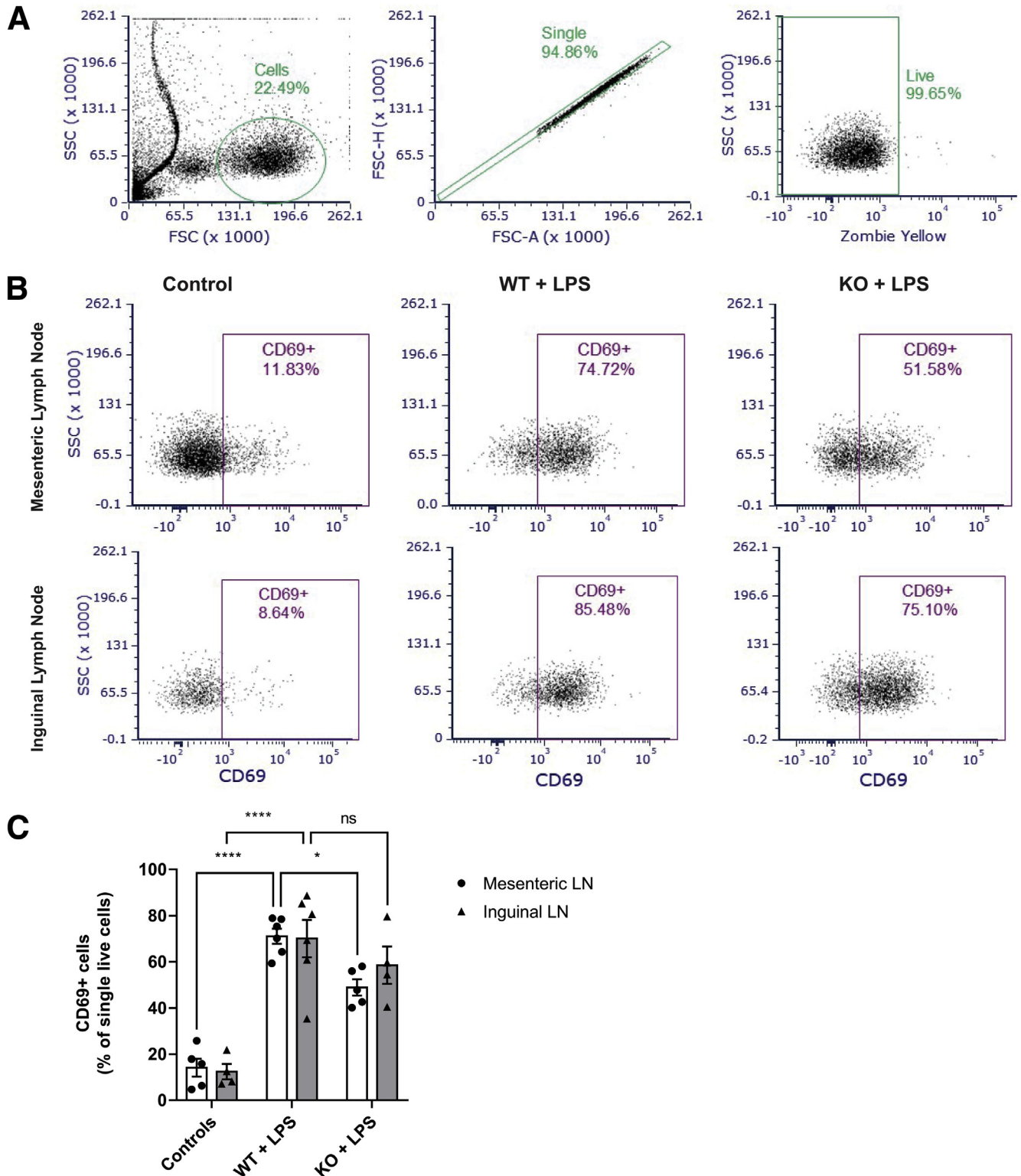


Figure 4. Enteric glial MHC-II signaling contributes to IFN γ /LPS-induced immunocyte activation in mesenteric lymph nodes. (A) Flow cytometry gating strategy to select cells based on the appropriate forward scatter (FSC) and side scatter (SSC) (left); single events based on the FSC area (FSC-A) and height (FSC-H) (middle); and live cells without the Zombie Yellow viability dye (right). (B) Representative data of an early activation marker CD69 expression in cells from the mesenteric (top row) and inguinal lymph nodes (bottom row) that were harvested from mice treated with IFN γ and saline (control are pooled glial^{MHC2KO} animals and wild-type littermates, left column), IFN γ - and LPS-treated wild-type littermates (WT + LPS, middle column), and IFN γ - and LPS-treated glial^{MHC2KO} mice (WT + knockout [KO], left column). (C) Percentage of single live cells expressing CD69 in the mesenteric and inguinal lymph nodes of glial^{MHC2KO} animals (KO) and wild-type littermates (WT) before (controls) and after LPS stimulation (n = 4–6 mice); 2-way analysis of variance with Sidak's-corrected multiple comparisons; ^{ns}P = .424, *P = .022, and ****P < .0001. LN, lymph node.

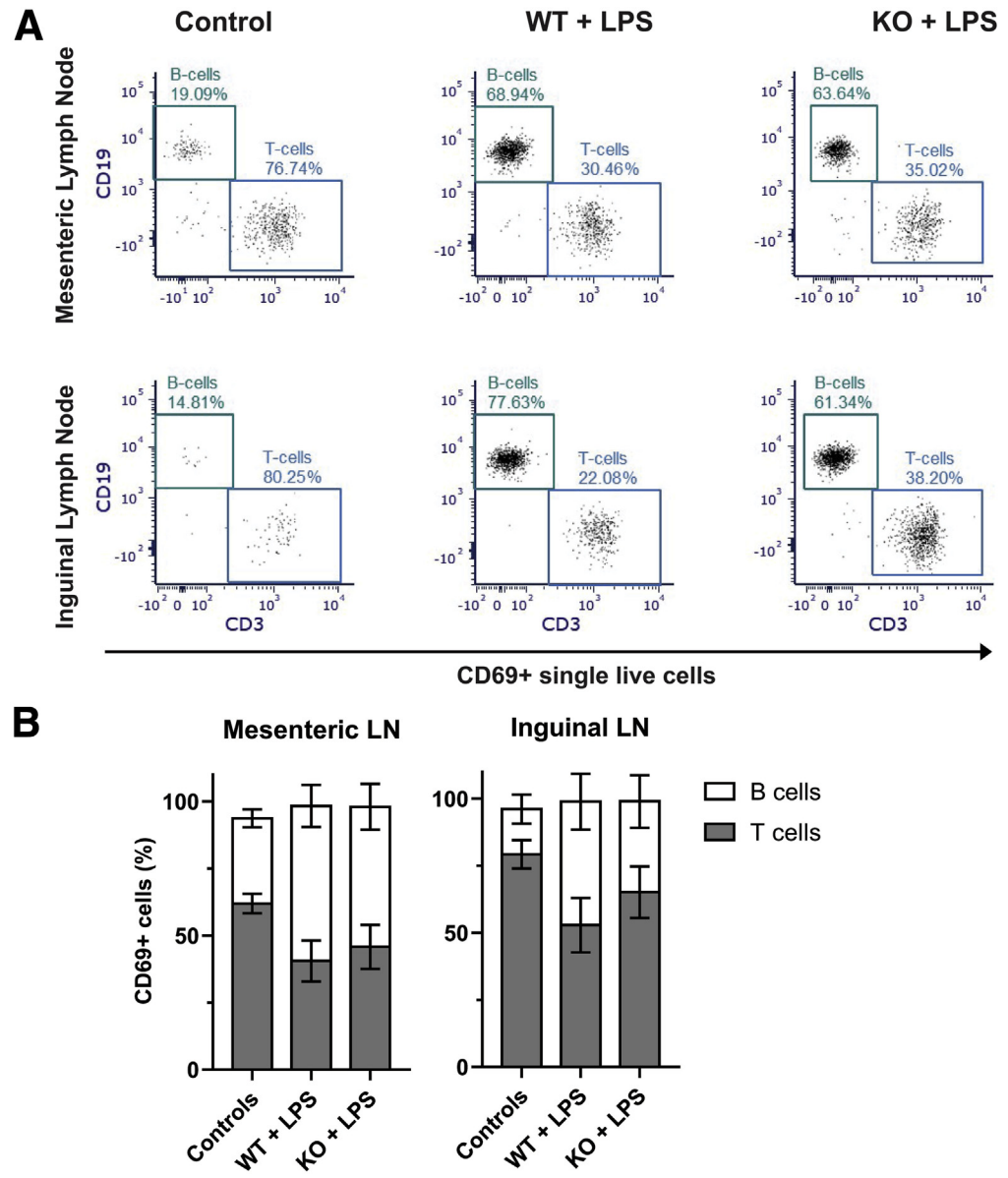


Figure 5. LPS-activated lymph node (LN) cells are lymphocytes composed of similar proportions of B and T cells. (A) Expression of CD3 and CD19, markers of B and T cells, in CD69⁺ single live cells from the mesenteric (*top row*) and inguinal lymph nodes (*bottom row*) that were harvested from mice treated with IFN γ and saline (control, *left column*), IFN γ - and LPS-treated wild-type littermates (wild-type [WT] + LPS, *middle column*), and IFN γ - and LPS-treated glial^{MHC2KO} mice (WT + knockout [KO], *left column*). (B) Percentage of CD69⁺ single live cells expressing either B-cell marker CD19 or T-cell marker CD3 in the mesenteric (*left*) and inguinal (*right*) lymph nodes of glial^{MHC2KO} animals (KO) and wild-type littermates (WT) before (controls) and after LPS stimulation ($n = 4-7$ mice).

whether a specific T-lymphocyte subtype is affected preferentially by glial MHC-II. The baseline activated proportions of T-lymphocyte subtypes expressing CD69 in IFN γ + saline-treated wild-type control animals were 66% \pm 25% of IFN γ ⁺ cells, 48% \pm 21% of IL4⁺ cells, 46% \pm 11% of IL17⁺ cells, and 43% \pm 14% of FoxP3⁺ cells (Figure 7A). Challenge with IFN γ and LPS in wild-type animals did not change the activated portion of IFN γ ⁺ or IL4⁺ cells, but significantly increased the activated portions of IL17⁺ ($P = .0025$) and FoxP3⁺ ($P = .0121$) cells to 83% \pm 8% and 77% \pm 13%, respectively (Figure 7A). Glial MHC-II ablation in stimulated animals did not significantly alter the activated portions of IFN γ ⁺ or IL4⁺ cells, but significantly decreased the activated portions of IL17⁺ ($P = .0021$) and FoxP3⁺ ($P = .0057$) cells to levels comparable with healthy wild-type controls treated with IFN γ + saline. Glial MHC-II

ablation in control animals had no effect on T-lymphocyte subtype activation. Taken together, these results show that enteric glial MHC-II primarily affects the activation state of Th17 and T_{reg} subtypes within the CD4⁺ population of T-lymphocytes in mesenteric lymph nodes.

Given the major effect of glial MHC-II ablation on T-lymphocyte activation in mesenteric lymph nodes, we wondered if local Sox10⁺ cells might exist within mesenteric lymph nodes that would be susceptible to MHC-II ablation and mediate the observed effects. We assessed this possibility by using Sox10^{CreERT2}^{+/+};tdTomato reporter mice to screen for potential Sox10⁺ cells in the mesenteric lymph nodes. We did not detect any tdTomato-expressing Sox10⁺ cells within mesenteric lymph nodes in either resting conditions or when stimulated with IFN γ and LPS (data not shown). The absence of Sox10⁺ cells in

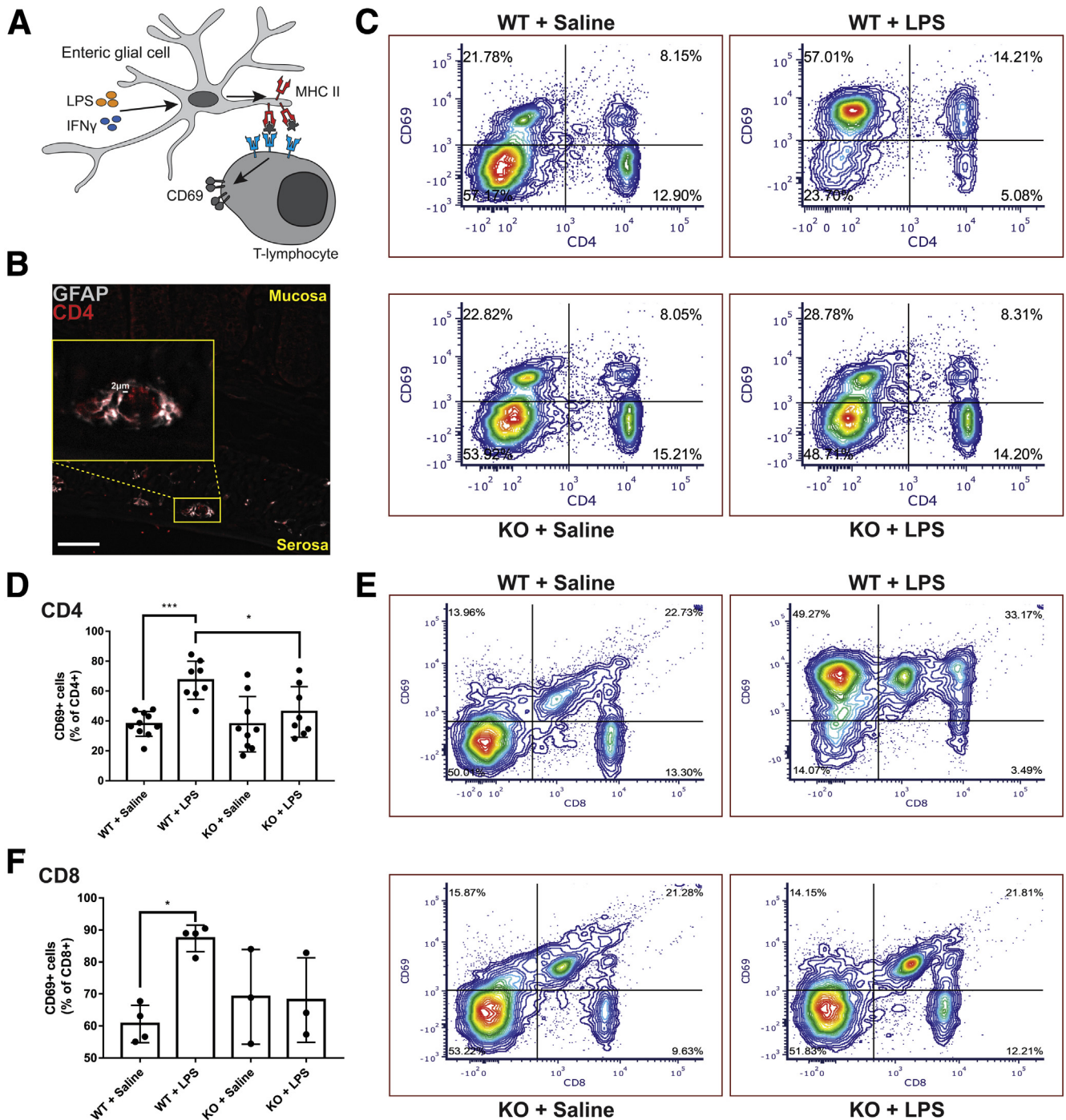


Figure 6. Enteric glial MHC-II expression affects T-lymphocyte activation. (A) Schematic showing enteric glia expressing MHC-II when stimulated with IFN γ and LPS. MHC-II molecules interact with T-lymphocytes and cause changes in activation state as measured by CD69 expression. (B) Representative image of GFAP (grey) and CD4 (red) immunofluorescent labeling in a colon cross-section showing the close proximity of CD4-expressing T-lymphocytes with GFAP expressing enteric glia in the myenteric plexus. Scale bar: 50 μ m. (C) Representative flow cytometric contour plots of mesenteric lymph nodes labeled with CD4 and CD69 in glial^{MHC2KO} (knockout [KO]) and wild-type (WT) littermates pretreated with IFN γ and then challenged with LPS or saline control. The proportion of total gated cells in each quadrant is expressed as a percentage. (D) Levels of activated CD4⁺ cells quantified as a percentage of total CD4⁺ cells that are CD4⁺CD69⁺ (n = 8–10 mice). (E) Representative contour plots of mesenteric lymph nodes labeled with CD8 and CD69. Proportions of gated cells in each quadrant are expressed as a percentage. (F) Proportion of total CD8⁺ T-lymphocytes expressing CD69 quantified in each treatment condition (n = 3–4 mice). Two-way analysis of variance with Tukey-corrected multiple comparisons; * $P < .05$, *** $P < .001$.

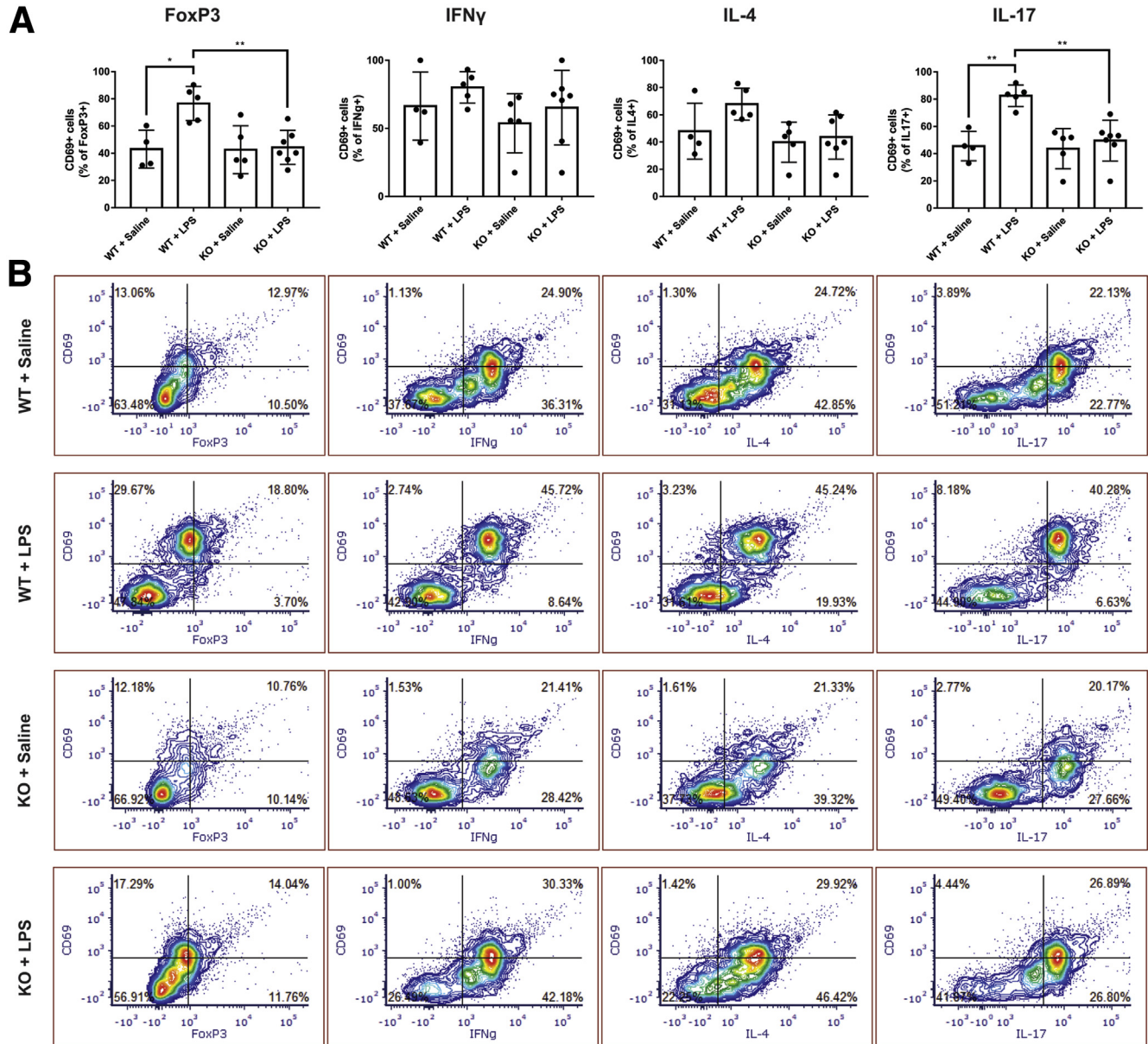


Figure 7. Enteric glial MHC II expression affects FoxP3⁺ and IL17⁺ cell populations to a greater degree than IFN γ ⁺ and IL4⁺ cell populations. (A) Levels of activated IFN γ ⁺, IL4⁺, IL17⁺, or FoxP3⁺ cells quantified as a percentage of total subtype-marker-expressing cells that also express CD69 ($n = 4-7$ mice). Two-way analysis of variance with Tukey-corrected multiple comparisons; * $P < .05$, ** $P < .005$). (B) Representative contour plots of mesenteric lymph nodes of each label are listed in corresponding columns. Proportion of total gated cells in each quadrant expressed as a percentage.

mesenteric lymph nodes suggests that changes in the T-lymphocyte activation state are the result of changes in enteric glial MHC-II expression in the intestine and not other cell types residing in the mesenteric lymph node.

Enteric Glia Affect Local, but Not Serum or Colonic, Cytokine Levels

Enteric glia express proinflammatory cytokines when stimulated with IFN γ and LPS in vitro,¹⁵ and these cytokines may play a role in activating nearby T-lymphocytes. Therefore, we isolated glial ribosomal-associated RNA in

Sox10^{CreERT2}/+/-;RiboTag mice and used a NanoString (NanoString, Seattle, WA) gene array (Table 1) to examine expression of select genes of interest (Table 1, Figure 8A). We tested whether enteric glia alter their expression of cytokines in response to IFN γ and LPS. Compared with control animals treated with IFN γ + saline, treatment with IFN γ + LPS elicited changes in several genes (Figure 8A). Most glial cytokines assessed were not affected significantly at the genomic level by IFN γ and LPS (Figure 8B). However, *Il1a* was increased significantly ($P = .0001$) and *Il12b* was decreased significantly ($P = .0032$). These minor changes in glial cytokine responses suggest that glial MHC-II expression

Table 1. Genes Investigated by Custom NanoString Panel

Gene type	Gene name	Gene symbol
	Glial fibrillary acidic protein	Gfap
Glial genes	S100 protein	S100b
Neuronal genes	Synaptophysin RNA binding protein (NeuN)	Syp Rbfox3
Macrophage genes	CD68 antigen Adhesion G protein-coupled receptor E1 (F4/80)	Cd68 Adgre1
Phagocytosis genes	CD36 antigen C-type lectin domain family 7 Collectin subfamily member 12 Ficolin A Ficolin B ^a Multiple EGF-like-domains 10 Platelet endothelial aggregation receptor 1 Engulfment adaptor PTB domain Stabilin 2 Milk fat globule-EGF factor 8 Tubby-like protein 1	CD36 Clec7A Colec12 Fcn1 Fcn2 Megf10 Pear1 Gulp1 Stab2 Mfge8 Tulp1
Antigen processing and presentation genes	Cathepsin B Class II transactivator Histocompatibility 2, class II antigen A, β 1 Histocompatibility 2, class II, locus Dma Cathepsin L CD40 antigen CD80 antigen CD86 antigen Lysosomal-associated membrane protein 1 Lysosomal-associated membrane protein 2 Toll-like receptor 2 Toll-like receptor 4	Ctsb Ciita H2-Ab1 H2-Dma Ctsl Cd40 Cd80 Cd86 Lamp1 Lamp2 Tlr2 Tlr4
Cytokines	Interleukin 1 Interleukin 2 Interleukin 4 Interleukin 6 ^a Interleukin 8 ^a Interleukin 12A Interleukin 12B Interleukin 18 Interleukin 23, α subunit p19 Transforming growth factor β Tumor necrosis factor α Interferon γ Lymphocyte activation gene 3 Lymphotoxin A Lymphotoxin B Neutrophil cytosolic factor 1	Il1 Il2 Il4 Il6 Il8 Il12a Il12b Il18 Il23a Tgfb1 Tnf Ifng Lag3 Lta Ltb Ncf1
Internal reference genes	Alanyl-tRNA synthetase Ankyrin repeat and SOCS box-containing 10 Coiled-coil domain containing 127 CCR4-NOT transcription complex, subunit 10 Casein kinase 2, α prime polypeptide Family with sequence similarity 104, member A Glucuronidase, β Leucyl-tRNA synthetase Mitochondrial tRNA translation optimization 1 Suppressor of Ty 7-like Transcriptional adaptor 2B TATA box binding protein X-prolyl aminopeptidase (aminopeptidase P) 1, soluble	Aars Asb10 Ccdc127 Cnot10 Csnk2a2 Fam104a Gusb Lars Mto1 Supt7l Tada2b Tbp Xpnpep1

NOTE. Selected genes in pathways related to phagocytosis, antigen processing and presentation, and cytokines. CCR4, C-C Motif Chemokine Receptor 4; EGF, Epidermal growth factor; PTB, Polypyrimidine Tract Binding Protein; SOCS, Suppressor of cytokine signaling; tRNA, transfer ribonucleic acid. Glial, neuronal, macrophage, and internal reference genes were used as controls.

^aGenes that did not pass NanoString panel quality control and were not included in the analysis. Glial, neuronal, macrophage, and internal reference genes were used as controls.

Table 2. Primary and Secondary Antibodies Used

Antigen target	Host species	Dilution	Final antibody concentration	Conjugate	Manufacturer	Product number	RRID	Lot number
GFAP	Chicken	1:1000	19.4 $\mu\text{g/mL}$	N/A	Abcam (Cambridge, MA)	ab4674	AB_304558	GR3368950-2
MHC-II	Rat	1:200	5 $\mu\text{g/mL}$	N/A	Novus Biologicals (Centennial, CO)	NBP2-21789	AB_2828034	529699
CD74	Rabbit	1:200	5 $\mu\text{g/mL}$	N/A	Bioss Antibodies (Woburn, MA)	BS-2518R	AB_10857560	AG10193417
P62	Rabbit	1:200	2.15 $\mu\text{g/mL}$	N/A	Abcam (Cambridge, MA)	ab109012	AB_2810880	GR3241806-2
LC3B	Rabbit	1:200	4.19 $\mu\text{g/mL}$	N/A	Abcam (Cambridge, MA)	ab192890	AB_2827794	GR3264793-8
Anti-HA-Tag (C29F4)	Rabbit	1:500	0.13 $\mu\text{g/mL}$	N/A	Cell Signaling Technology (Danvers, MA)	3724	AB_1549585	B222922 / B272772
HuC/HuD	Mouse	1:200	1 $\mu\text{g/mL}$	Biotinylated	Thermo Fisher Scientific (Waltham, MA)	A-21272	AB_2535822	2126799
Anti-chicken IgY	Goat	1:400	3.75 $\mu\text{g/mL}$	Dylight405	Jackson ImmunoResearch (West Grove, PA)	103-475-155	AB_2337389	124380
Anti-rat IgG	Goat	1:400	3.75 $\mu\text{g/mL}$	AlexaFluor 594	Jackson ImmunoResearch (West Grove, PA)	112-585-003	AB_2338372	105385
Anti-rabbit IgG	Goat	1:400	5 $\mu\text{g/mL}$	AlexaFluor 488	Invitrogen (Waltham, MA)	A-11034	AB_2576217	1141875
Anti-mouse CD3	Rat IgG2b, κ	1:100	2 $\mu\text{g/mL}$	Brilliant Violet 421	BioLegend (San Diego, CA)	100228	AB_2562553	B311657
CD45.2	Mouse	1:200	2.5 $\mu\text{g/mL}$	AlexaFluor 488	BioLegend (San Diego, CA)	109816	AB_492868	B280505
CD4	Rat	1:200	2.5 $\mu\text{g/mL}$	FITC	BioLegend (San Diego, CA)	100509	AB_312712	B269033
CD8a	Rat	1:200	1 $\mu\text{g/mL}$	APC/Cy7	BioLegend (San Diego, CA)	100713/ 100714	AB_312752/ AB_312753	B283111/ B260276
Anti-mouse CD11b	Rat/IgG2b, κ	1:200	1 $\mu\text{g/mL}$	PerCP-eFluor 710	Thermo Fisher Scientific (Waltham, MA)	46-0112-82	AB_2866430	2336535
Anti-mouse CD11c	Armenian hamster IgG	1:100	2 $\mu\text{g/mL}$	PE	BioLegend (San Diego, CA)	117307	AB_313776	B301182
Anti-mouse CD19	Rat IgG2a, κ	1:100	2 $\mu\text{g/mL}$	APC	BioLegend (San Diego, CA)	115512	AB_313647	B284257
CD69	Armenian hamster	1:200	1 $\mu\text{g/mL}$	PE/Cy7	BioLegend (San Diego, CA)	104511/ 104512	AB_493565/ AB_493564	B291440/ B253212
IFN γ	Rat	1:100	2 $\mu\text{g/mL}$	PE	BioLegend (San Diego, CA)	505808	AB_315402	B265789
IL4	Rat	1:100	2 $\mu\text{g/mL}$	APC	BioLegend (San Diego, CA)	504105	AB_315319	B270118
IL17	Rat	1:20	10 $\mu\text{g/mL}$	Brilliant Violet 510	BioLegend (San Diego, CA)	506933	AB_2562668	B263584
FoxP3	Rat	1:100	5 $\mu\text{g/mL}$	Pacific Blue	BioLegend (San Diego, CA)	126410	AB_2105047	B274192
TruStain FcX (anti-mouse CD16/32)	Rat IgG2a, λ	1:100	5 $\mu\text{g/mL}$	N/A (Fc receptor block)	BioLegend (San Diego, CA)	101320	AB_1574975	B305040

Cy7, Cyanine7; Fc, Fragment, crystallizable; FITC, fluorescein isothiocyanate; FoxP3, Forkhead Box P3; HA, hemagglutinin; HuC/HuD, Hu-antigen C/Hu-antigen D; PerCP, Peridinin-Chlorophyll-Protein; RRID, Research Resource Identifiers.

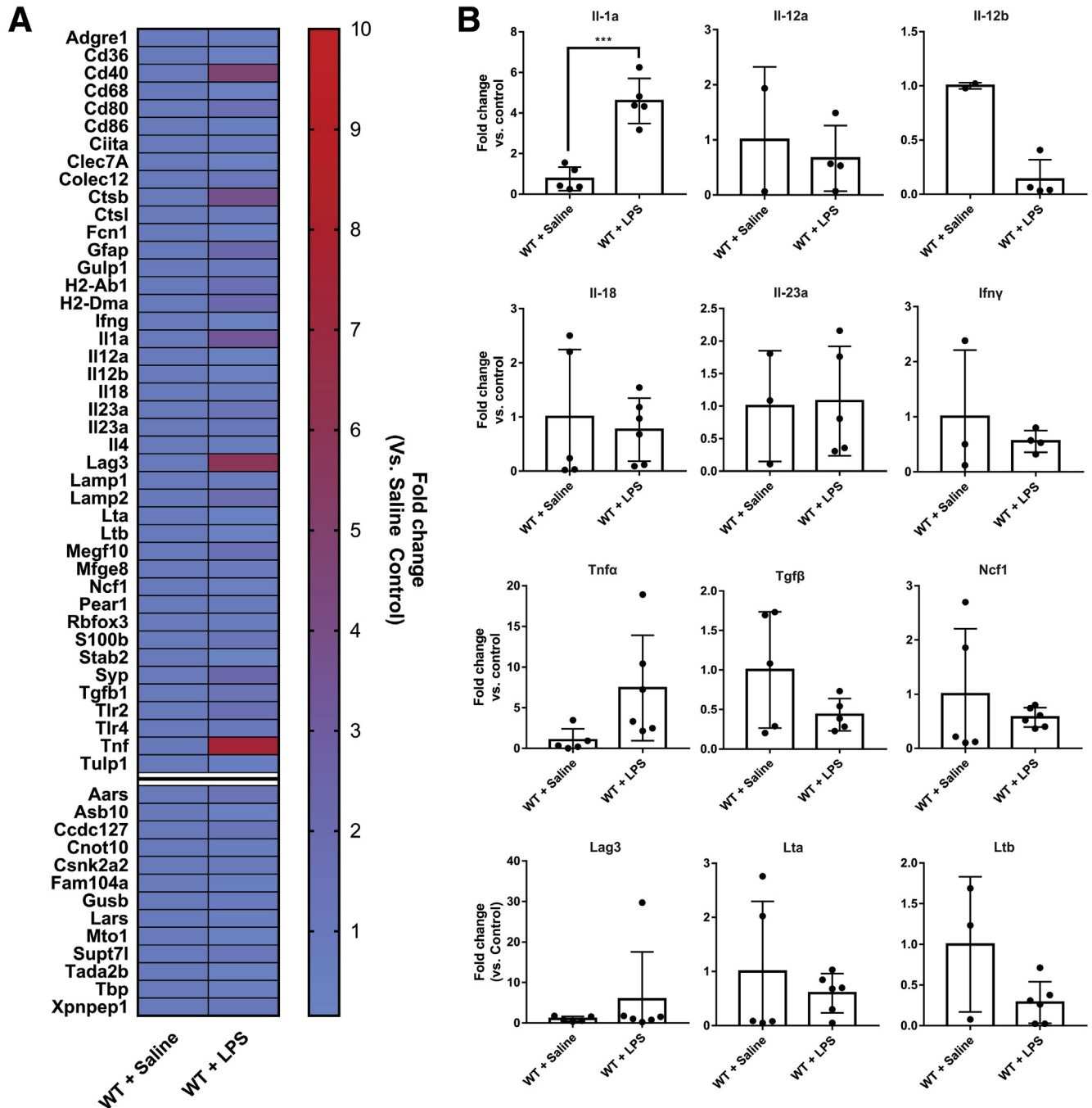


Figure 8. Enteric glial gene expression. (A) Heat map showing NanoString-quantified gene expression fold change in RiboTag animals stimulated with IFN γ + LPS compared with controls treated with IFN γ + saline. Genes represented in heatmap list correspond to phagocytosis, antigen presentation, and cytokine-related genes. Separated lower 13 genes represent internal reference genes. (B) Gene expression of select cytokines/chemokines in RiboTag animals stimulated with IFN γ + LPS or controls treated with IFN γ + saline ($n = 2-6$ mice). Unpaired Student t test; *** $P < .0005$. WT, wild-type.

plays a more prominent role in dictating T-lymphocyte activation than glial cytokine release under these conditions.

Because enteric glial MHC-II expression status alters T-lymphocyte activation and activated T-lymphocytes affect tissue and serum cytokine levels, we examined whether enteric glial MHC-II expression alters cytokine levels as a downstream effect via a bead-based multiplex enzyme-

linked immunosorbent assay. Most molecules examined in a panel of 31 cytokines and chemokines were not affected significantly by the IFN γ and LPS challenge in colonic tissue (Figure 9B) or serum (Figure 9C). However, significant increases were observed in colonic tissue levels of leukemia inhibitory factor and CCL5 (Figure 9B), and serum levels of granulocyte colony-stimulating factor, macrophage

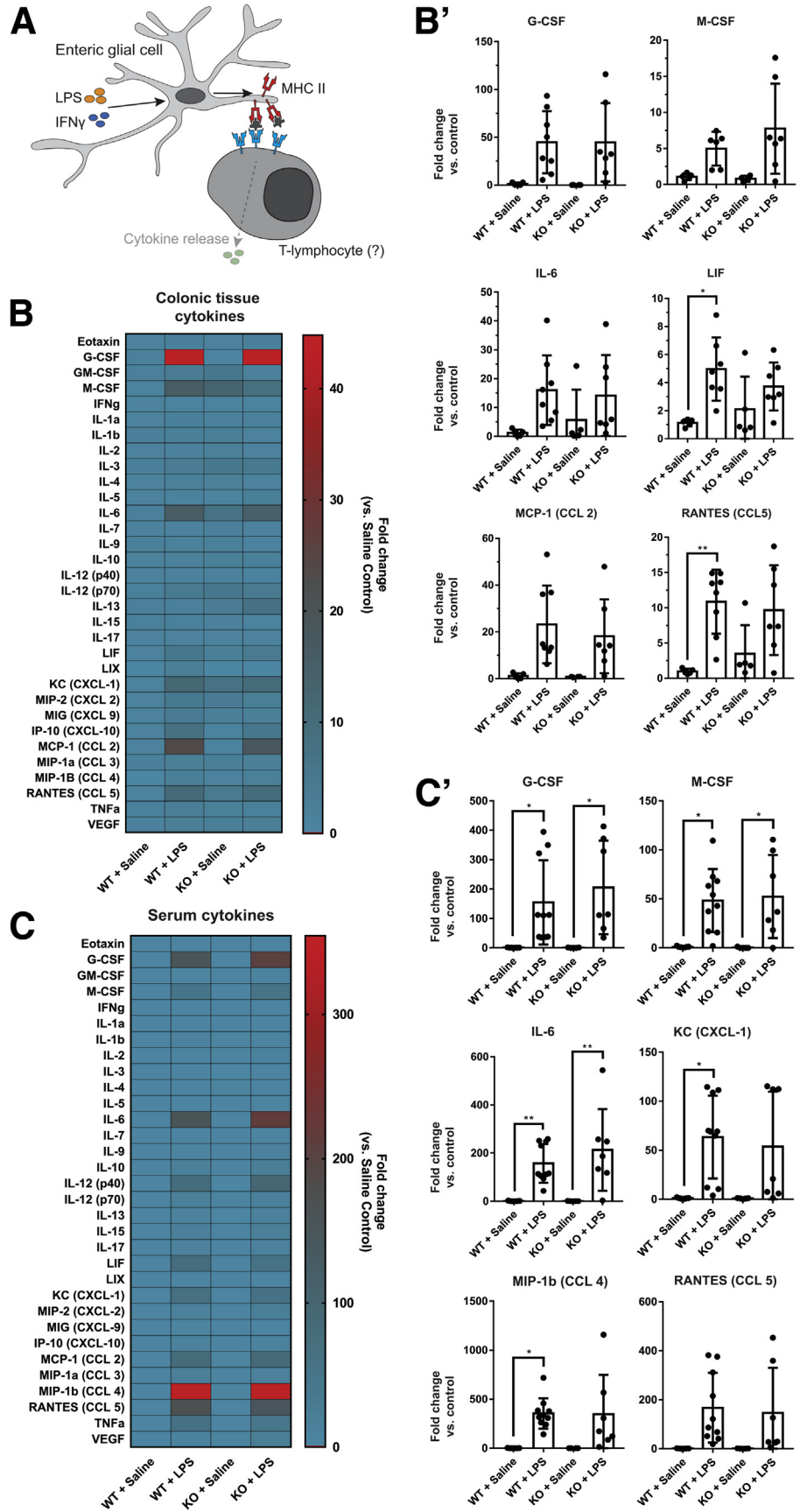


Figure 9. Enteric glial MHC-II expression has limited effects on serum and colonic tissue cytokine levels. (A) Schematic showing potential source of cytokine release from T-lymphocytes after activation via binding enteric glial MHC-II. (B) Heat map showing fold change compared with saline controls in quantified cytokines and chemokines in colonic tissue homogenates of male mice in glial^{MHC2KO} (knockout [KO]) and wild-type littermates pretreated with IFN γ and then challenged with LPS or saline control (n = 4–10 mice). Select tissue cytokines are presented in (B'). (C) Heat map showing fold change compared with saline controls in quantified cytokines and chemokines in serum samples of male mice (n = 4–8 mice). Select serum cytokines are presented in (C'). *P < .05, **P < .005. CCL, C-C motif ligand; CXCL, C-X-C motif ligand; G-CSF, Granulocyte colony-stimulating factor; GM-CSF, Granulocyte macrophage colony-stimulating factor; KC, Keratinocyte-derived chemokine; IP, Interferon-gamma-induced protein; LIF, Leukemia inhibitory factor; LIX, Lipopolysaccharide-induced CXC chemokine; MCP, Monocyte chemoattractant protein; M-CSF, Macrophage colony-stimulating factor; MIP, Macrophage inflammatory protein; RANTES, Regulated upon activation, normal T cell expressed and secreted; WT, wild-type.

colony-stimulating factor, IL6, keratinocyte-derived chemokine (C-X-C motif chemokine ligand 1), and macrophage inflammatory protein-1 β (C-C motif chemokine ligand 4) (Figure 9C). Ablating enteric glial MHC-II had little effect on colonic and serum cytokine levels, and expression in glial^{MHC2KO} animals did not differ significantly from wild-type animals (Figure 9B and C). Therefore, although glial antigen presentation does affect the activation profiles of immune cells in mesenteric lymph nodes, serum and regional cytokine profiles are driven mainly by other immune cells in this model.

It is possible that the lack of effects on serum cytokines in glial^{MHC2KO} mice is complicated by also ablating MHC-II in Sox10+ glia in the spleen.¹⁶ In agreement with prior work, we observed that Sox10+ spleen glia do express MHC-II (Figure 10A–D). However, the vast majority of MHC-II-expressing cells in spleen do not express Sox10, with Sox10-expressing cells having a density of 1.5 cells/mm² in splenic tissue sections. Therefore, it is unlikely that MHC-II ablation in Sox10+ cells of the spleen has a major impact that would confound our cytokine measurements in the serum.

Proinflammatory Stimuli IFN γ and LPS Do Not Trigger Phagocytosis in Enteric Glia

The effects of glial MHC-II on T-lymphocyte activation state suggest that glial MHC-II molecules are functional. In professional antigen-presenting cells, peptides loaded onto MHC-II are derived typically from the phagocytosis and processing of foreign antigens.¹³ We tested whether enteric glia present phagocytosed antigens onto MHC-II molecules by first examining the phagocytic potential of enteric glia (Figure 11A). Exposure to pHrodo BioParticles (Waltham, MA) elicited phagocytosis in CD45+ immune cells neighboring enteric ganglia (Figure 11C), but phagocytosis or internalization of labeled *Escherichia coli* particles was never observed in tdTomato+ enteric glia in 18 separate experiments (Figure 11B and C). We reasoned that this lack of effect might be the result of using pHrodo-labeled *E coli* particles as the phagocytic substrate and that glia might engulf material through other mechanisms such as endocytosis. Therefore, we used labeled LPS molecules and 1.0- μ m fluorescent polystyrene microspheres to test whether TLR4-mediated endocytosis or size are contributing factors to glial phagocytosis. Incubation with fluorescently labeled LPS or fluorescent polystyrene microspheres did not elicit any uptake within enteric glial cells (Figure 11D), suggesting that enteric glia are either incapable of phagocytosis or that there is insufficient stimulation to trigger phagocytic behavior in enteric glia. Taken together, our results show that expression of MHC-II molecules on enteric glia when stimulated with low-dose IFN γ and LPS is not the result of the phagocytosis of foreign antigens, but is derived from other pathways.

Glial Autophagy Regulates MHC-II Expression

Our data show that glial MHC-II expression occurs independently of phagocytosis. Therefore, we examined

alternative pathways for MHC-II induction. In antigen-presenting cells such as B cells, a deficiency in autophagic protein Atg5 decreases MHC-II expression levels, suggesting that autophagy regulates MHC-II expression levels in antigen-presenting cells.¹⁷ We tested whether a similar autophagy mechanism controls enteric glial MHC-II expression by measuring levels of the autophagy proteins p62 and LC3 over a 16-hour time course. As described earlier, MHC-II expression was detected in enteric glia by 4 hours after injection (Figure 12B). Expression of autophagic proteins LC3 and p62 is not limited to enteric glia and is distributed in both enteric neurons and glia. The punctate nature of LC3 labeling shows a greater density in enteric glia, while p62 labeling is more prominent in neurons compared with glia, consistent with findings in single-cell RNA-sequencing databases¹² (Figure 12B and C). Glial MHC-II expression significantly ($P = .0021$) increased by 8 hours after injection with IFN γ and LPS and further increased by 16 hours ($P < .0001$) (Figure 12B–D). LC3+ puncta density in both enteric glia (Figure 12F) and enteric neurons (Figure 12I) trended toward increased levels over 16 hours, while p62 expression was increased significantly in enteric glia ($P = .0060$) and neurons ($P = .0270$) by 4 hours after injection and subsequently decreased to pre-injection levels by 16 hours (Figure 12E and H). The spike and subsequent decrease in p62 labeling, with the concurrent trend in increasing LC3 puncta over 16 hours suggests that autophagy is active in both enteric glia and neurons.¹⁸ The timing of MHC-II up-regulation in enteric glia coincides with autophagy-mediated consumption of p62 molecules and accumulation of LC3 deposits, showing that enteric glial MHC-II expression occurs concurrently with autophagy pathways.

Because autophagy can lead to the presentation of intracellular antigens on MHC-II molecules,¹⁹ we tested whether our findings are indicative of autophagy-induced glial MHC-II expression. We used a combination of IFN γ and LPS, the autophagy stimulator rapamycin, and the autophagy inhibitor 3-methyladenine (3-MA) to test the regulation of glial MHC-II expression by autophagy. A 16-hour incubation with IFN γ and LPS significantly ($P = .0015$) increased MHC-II levels in enteric glia compared with untreated control animals, similar to our in vivo findings (Figure 12G). Combining IFN γ and LPS with rapamycin further increased glial the MHC-II expression level compared with untreated controls ($P < .0001$), but, interestingly, incubation with rapamycin alone did not increase MHC-II levels compared with control ($P = .8354$) (Figure 12G). However, tissues incubated with a combination of IFN γ , LPS, and 3-MA, or IFN γ , LPS, rapamycin, and 3-MA, had significantly decreased levels of glial MHC-II expression compared with non-3-MA-treated counterparts ($P = .0047$ and $P < .0001$, respectively) and reduced glial MHC-II expression to levels comparable with untreated controls (Figure 12G). Taken together, our data show that inhibition of glial autophagy effectively eliminates MHC-II labeling, suggesting that glial MHC-II expression requires autophagy activation. However, the inability for rapamycin alone to induce glial MHC-II suggests that the activation of

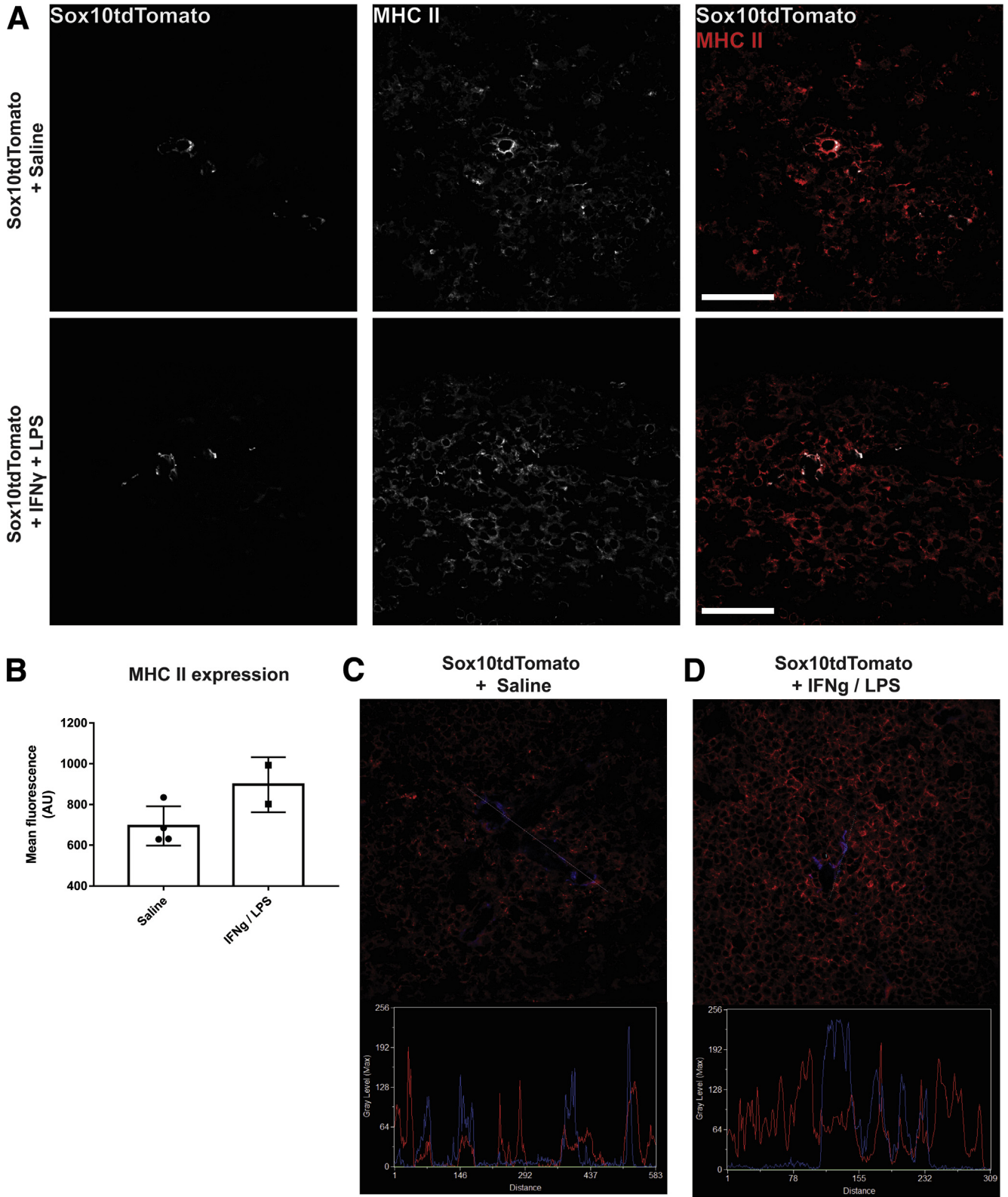


Figure 10. Sox10-expressing cells are present in sparse numbers in spleen tissue and express MHC-II. (A) Representative confocal images of tdTomato (white) and MHC-II (red) immunofluorescent labeling in spleen sections in IFN γ + LPS-treated and control animals. (B) Quantified MHC-II mean fluorescent intensity in Sox10tdTomato-expressing cells. Line-scan of MHC II (red)- and Sox10tdTomato (blue)-labeled spleen tissue from (C) control or (D) IFN γ + LPS-treated mice. Scale bars: 50 μ m. Max, maximum.

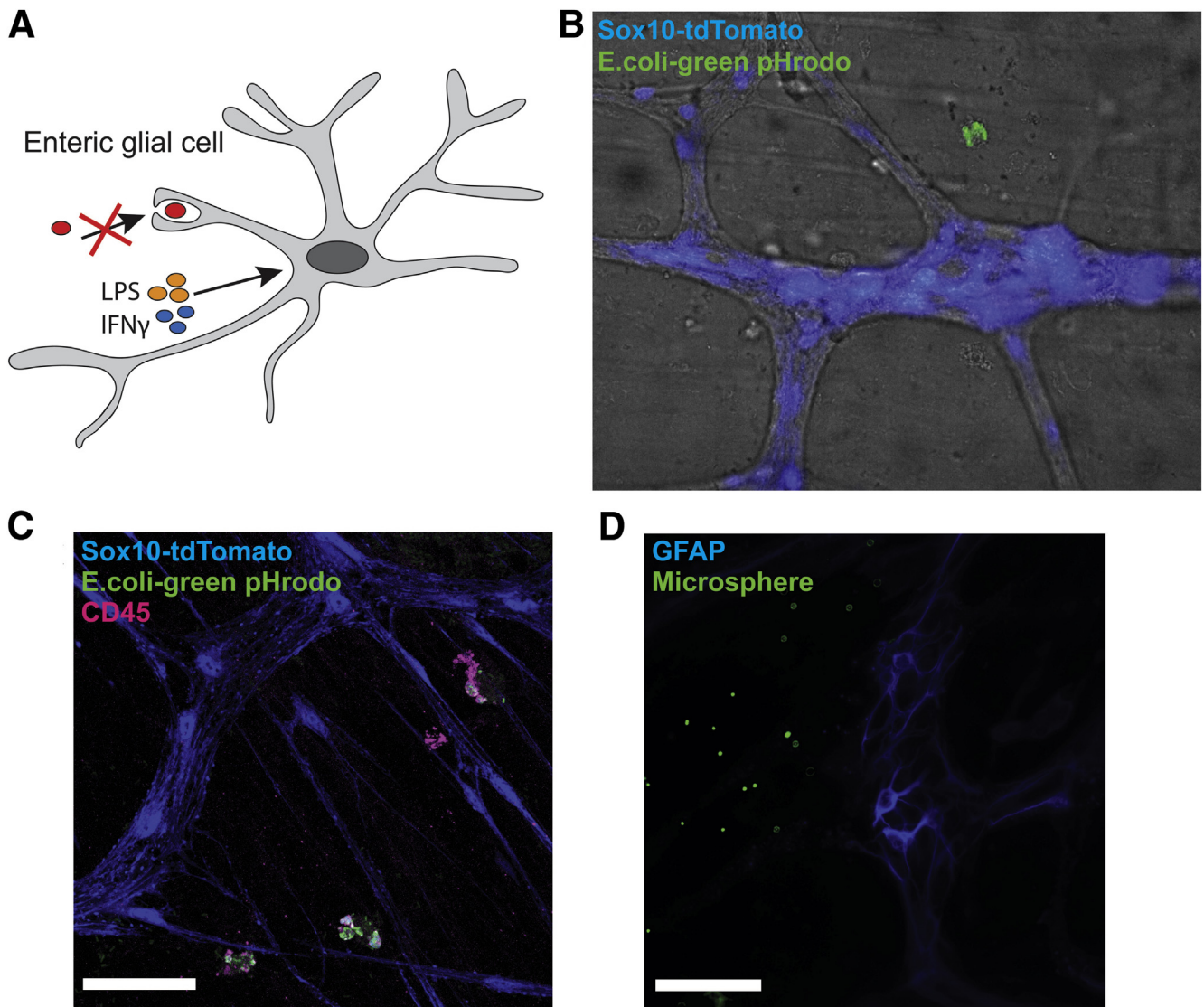


Figure 11. Enteric glia do not show phagocytic activity when stimulated with IFN γ and LPS. (A) Schematic showing that enteric glial cells do not show phagocytic activity when stimulated with IFN γ and LPS. (B) Representative brightfield and epifluorescent image of tdTomato-expressing Sox10 $^{+}$ cells (blue) and pHrodo-labeled *E coli* BioParticles (green). (C) Representative confocal image of tdTomato-expressing Sox10 $^{+}$ cells (blue), pHrodo-labeled *E coli* BioParticles (green), and CD45 immunolabeling (magenta). (D) Representative epifluorescence image of GFAP-expressing enteric glia (blue) and fluorescently labeled polystyrene microspheres (green). Scale bars: 50 μ m.

autophagy alone is insufficient to trigger glial MHC-II expression.

Discussion

The notion that enteric glia function as antigen-presenting cells stems from observations in Crohn's disease and Chagas disease, in which glia increase MHC-II expression.^{6,8} The functional significance of these observations has remained in question ever since. Here, we show that antigen presentation by enteric glia is associated with the activation of B and T-lymphocytes. Enteric glia are sensitive to inflammatory stimuli and respond to low-dose IFN γ and LPS by expressing MHC-II molecules. Enteric glial MHC-II molecules are functional and contribute to

CD4 $^{+}$ T-lymphocyte activation, particularly in the Th17 and T_{reg} subpopulations. These effects do not involve large shifts in proinflammatory mediators. Glial MHC-II expression is not phagocytosis-mediated but instead is dependent on autophagy activation. However, autophagy activation alone is not sufficient to elicit glial MHC-II expression.

MHC-II is expressed primarily by professional antigen-presenting cells and plays an important role in their interactions with T-lymphocytes. We show that enteric glia express MHC-II in an inducible manner when exposed to proinflammatory stimuli, consistent with prior *in vitro* and *in vivo* human studies that have shown that glial MHC-II expression is induced by enteroinvasive *E coli* or inflammation.⁶⁻⁸ Furthermore, the punctate distribution of MHC-II along glial processes is consistent with findings in Chagas

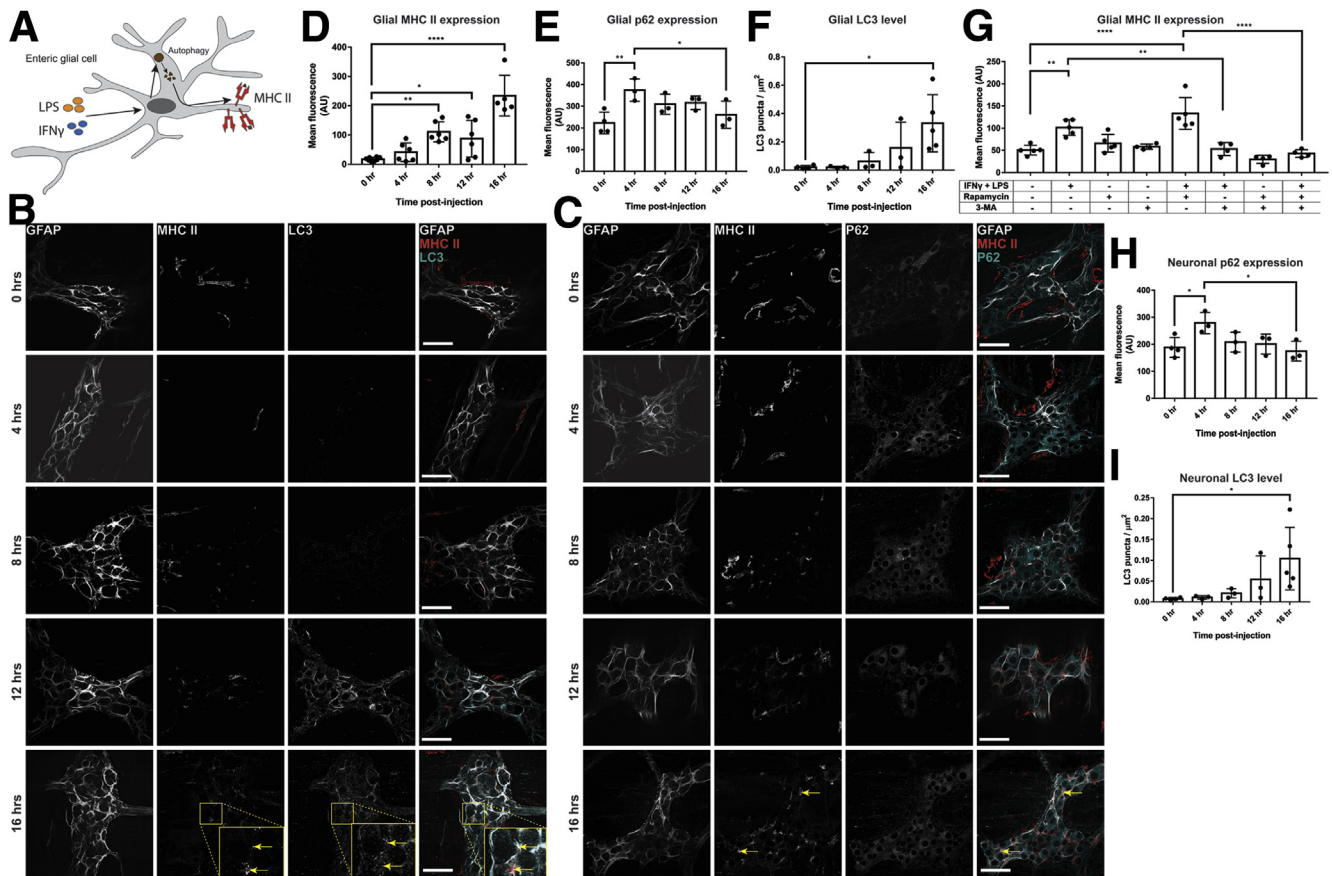


Figure 12. Enteric glia express MHC-II via autophagy pathways. (A) Schematic showing enteric glial MHC-II loading and expression of autophagy-derived peptides when stimulated with IFN γ and LPS. (B) Representative confocal images of GFAP (grey), MHC-II (red), and LC3 (cyan) immunofluorescent labeling in enteric ganglia in wild-type animals injected with IFN γ and LPS over a 16-hour time course. LC3 show punctate labeling and are distributed in a neuronal and glial pattern. Yellow arrows highlight colocalization of MHC-II, LC3, and GFAP. (C) Representative confocal images of GFAP (grey), MHC-II (red), and P62 (cyan) immunofluorescent labeling in enteric ganglia in wild-type animals injected with IFN γ and LPS over a 16-hour time course. P62 labeling is prominent in enteric neurons but is distributed in both neurons and glia. Scale bars: 50 μ m. Yellow arrows highlight colocalization of MHC-II and GFAP. (D and E) Quantified mean fluorescent intensity of MHC-II and p62 labeling on GFAP-expressing enteric glia in the myenteric plexus. Wild-type animals were injected with IFN γ and LPS and colons were harvested over a 16-hour time course ([D] $n = 5-8$ mice and [E] $n = 3-4$ mice). (F) Quantified density of LC3 puncta labeling over the area of GFAP-expressing enteric glia in the myenteric plexus. Wild-type animals were injected with IFN γ and LPS and colons were harvested over a 16-hour time course ($n = 3$ mice). One-way analysis of variance with Sidak-corrected multiple comparisons. (G) Quantified mean fluorescent intensity of MHC-II labeling on GFAP-expressing enteric glia in the myenteric plexus. Longitudinal muscle-myenteric plexus tissue preparations from wild-type animals were incubated with a combination of IFN γ and LPS, rapamycin, and 3-MA for 16 hours before fixation and immunolabeling ($n = 4-5$ mice). (H) Quantified mean fluorescent intensity of p62 labeling within enteric ganglion outside of GFAP-expressing enteric glia in the myenteric plexus. Wild-type animals were injected with IFN γ and LPS and colons were harvested over a 16-hour time course ($n = 3-4$ mice). One-way analysis of variance with Sidak-corrected multiple comparisons. (I) Quantified density of LC3 puncta labeling within enteric ganglion outside of GFAP-expressing enteric glia in the myenteric plexus. Wild-type animals were injected with IFN γ and LPS and colons were harvested over a 16-hour time course ($n = 3$ mice). One-way analysis of variance with Sidak-corrected multiple comparisons; * $P < .05$, ** $P < .005$, and **** $P < .0001$.

disease.⁶ In our study, enteric glia expressed MHC-II in the absence of inflammation or observable tissue damage. This suggests that glial antigen presentation may act as an early responder to inflammatory stress, consistent with observations in Crohn's disease showing that enteric glia express MHC-II in diseased areas, macroscopically uninvolved areas, and occasionally in healthy individuals.^{6,8} We did not observe glial MHC-II expression in control animals that were treated with IFN γ + saline and it was not observed in

cultured human enteric glia in vitro.⁷ This discrepancy in baseline glial MHC-II expression may be owing to the lack of a microbiome in vitro, and a murine tolerance to LPS and bacterial components.²⁰ However, baseline glial expression of MHC-II in human beings suggests that enteric glia constantly monitor the enteric nervous system (ENS) and the surrounding environment. Interactions with microbiome-derived antigens and secreted compounds may be important in regulating glial autophagy, similar to

microbiome interactions in other colonocytes.^{21,22} Microbiome composition therefore may modulate glial autophagy, immune activation, and homeostasis. Intestinal epithelial cell expression of MHC-II show similar anti-inflammatory effects by limiting Th1 cell infiltration and modulate T-lymphocyte subtype distribution in the intestine.²³

The presence of enteric glial MHC-II expression in vivo and in vitro⁶⁻⁸ and their ability to suppress T-lymphocyte proliferation in co-cultures⁴ suggest glial-T-lymphocyte recognition and interaction. However, the functional role of antigen presentation by enteric glia and their potential to influence T-lymphocytes in vivo is not understood. Here, we show that enteric glial MHC-II expression plays an important role in the activation of CD4+ T-lymphocytes in mesenteric lymph nodes. We also noted a surprisingly large population of CD4- cells expressing CD69 in stimulated animals. A portion of those cells responding to glial MHC-II represent CD69-expressing CD8+ T-lymphocytes,²⁴ with the remaining cells corresponding to CD19-expressing B-lymphocytes. Because the proportions of B-lymphocytes to T-lymphocytes in mesenteric nodes remain consistent between wild-type and glial^{MHC2KO} animals treated with IFN γ + LPS, our data show that activation of both T-lymphocytes and B-lymphocytes is affected by enteric glial MHC-II expression. Whether enteric glia interact with B-lymphocytes in a cell-to-cell manner similar to astrocytes, or via secreted compounds similar to microglia,²⁵ remain to be studied. The decreased CD8+ T-lymphocyte activation may contribute to the lack of histologic tissue damage. Our data show that glial MHC-II expression has a propensity to affect Th17 and T_{reg} subpopulations, rather than Th1 and Th2 subpopulations. This apparent conflict in immune regulation by activating both proinflammatory and anti-inflammatory T-lymphocyte subpopulations suggest a feedback inhibition to limit Th17 activity.²⁶ Alternatively, the Th17 subpopulation may show anti-inflammatory actions by secreting anti-inflammatory cytokines.²⁷ Furthermore, enteric glia may contribute to an anti-inflammatory phenotype by destabilizing interactions with certain T-lymphocyte subtypes to inhibit proliferation, similar to effects seen in dendritic cells.²⁸ Despite enteric glial MHC-II expression having no apparent effect on regional tissue cytokine levels, gene expression changes suggest that enteric glia may have a mixed role in the local ENS microenvironment by expressing *Il1a* while decreasing *Il12b*. The apparent expression of certain proinflammatory cytokines despite decreasing others may be owing to the concurrent activation of separate pathways. Although *Il1a* gene expression may be driven by direct binding of LPS molecules onto TLR4 receptors on enteric glia, a decrease in *Il12b* may be owing to the activation of other separate signaling pathways. In support, enteric glia show strong immunosuppressive effects that inhibit T-lymphocyte proliferation in co-culture models and this effect is strengthened in enteric glia derived from Crohn's patients.⁴ In contrast, enteric glia can contribute to neuronal cell death,²⁹ and cultured human enteric glia challenged with IFN γ and LPS increase gene expression of various proinflammatory

cytokines.¹⁵ This suggests that the dynamic immunomodulatory capabilities of enteric glia depend on the surrounding environment.

Our current data focus on the glial^{MHC2KO} (*Sox10*^{CreERT2}; *IAB*^{fl/fl}) model and its effects on T-lymphocytes of the mesenteric lymph nodes. Because we did not detect any Sox10+ cells that would be susceptible to MHC-II ablation in mesenteric lymph nodes, how enteric glia in the ENS affect T-lymphocyte activation while in separate anatomic locations remains to be understood. Given the proximity of local CD4+ T-lymphocytes to enteric glia, it is possible that enteric glia influence the activation of local T-lymphocytes via cell interactions or secreted compounds, and the migration of activated lymphocytes subsequently could have a wider-reaching effect in regional lymph nodes.⁴ Similarly, enteric glia potentially may influence nearby dendritic cells to bring about lymph node effects. Enteric glial expression of 15-deoxy- $\Delta^{12,14}$ -prostaglandin J₂³⁰ conceivably can influence dendritic cells to stimulate activation of type 1 regulatory T-lymphocytes,³¹ but this interaction has yet to be described.

Phagocytosis is an important pathway for professional antigen-presenting cells to uptake foreign antigens for processing and presentation. In our study, we did not find evidence that enteric glia uptake labeled *E coli*, labeled LPS, or fluorescent latex beads. The lack of phagocytosis in our study, however, may be owing to the strength of the proinflammatory stimuli used, because others successfully have shown phagocytic potential in related glial populations in the central nervous system.³² Therefore, stronger stimuli or nearby cell death may be necessary for enteric glia to show phagocytic activity. Given their shared characteristics with astrocytes, their proximity to enteric neurons, and their ability to contribute to neuronal demise,^{29,33} it is conceivable that enteric glia also uptake neuronal fragments during neuronal injury or death. The expression of enteric glial MHC-II in situations of inflammation and neuron loss, such as in Chagasic megacolon or Crohn's disease,^{6,8} suggest that enteric glia play a role in these disease states. Whether enteric glia contribute to neuronal death and inflammation through MHC-II expression or promote anti-inflammatory pathways to maintain homeostasis remains to be studied.

The ability of enteric glia to express MHC-II molecules in the absence of phagocytosis suggests that glia use alternative pathways to promote the loading of antigens onto MHC-II for presentation. Enteric glial MHC-II expression both depends and coincides with autophagy activation, which suggests the possibility that enteric glia present autophagy-derived peptides on their MHC-II molecules. However, mass spectrometry analysis of glial MHC-II molecules is necessary to determine the identity of presented peptides conclusively. Because no intestinal tissue damage, evidence of gliosis, or neuronal death was observed in conjunction with our study findings, autophagy activation in both enteric neurons and enteric glia may indicate a compensatory mechanism to limit potential inflammatory damage to the ENS. This potential

mechanism is indeed supported by findings from other groups showing that the activation of autophagy can inhibit intestinal inflammation and reduce colitis.³⁴ However, autophagy activation by rapamycin alone is insufficient to induce glial MHC-II expression. This may be owing to the nature of rapamycin having variable effectiveness in eliciting autophagy in different glial cell lines³⁵ or that enteric glia simply may require both a stimulus and a concomitant activation in autophagy to express MHC-II. However, the up-regulation of glial proinflammatory cytokine gene expression while also activating autophagy pathways suggest that 2 separate pathways may be activated concurrently by IFN γ and LPS challenge. Direct LPS binding onto enteric glial TLR4 receptors may contribute to a proinflammatory phenotype in enteric glia, while the activation of a separate pathway induces autophagy and an anti-inflammatory phenotype.

In conclusion, our results show that enteric glia respond to inflammatory stimuli by expressing functional MHC-II molecules to modulate T-lymphocyte activation. Furthermore, we show that autophagy activation is necessary, but insufficient, to induce enteric glial MHC-II expression (Figure 13). Together, these observations provide evidence for enteric glia being an important immune regulator during inflammatory stress and suggest that they may play an anti-inflammatory role during intestinal inflammation and inflammatory bowel disease to maintain homeostasis.

Materials and Methods

Animals

All protocols involving animals were approved by the Michigan State University Institutional Animal Care and Use Committee. Male and female C57BL/6 mice between 14 and 16 weeks old were used in all experiments. Animals were housed in ventilated cages with a 12-hour light-dark cycle, and access to food and water ad libitum. Mice with a conditional ablation of MHC-II in enteric glia (*Sox10^{CreERT2};IAB^{fl/fl}*) were generated in-house by breeding *Sox10^{CreERT2}/+* mice³⁶ (a gift from Dr Vassilis Pachnis, The Francis Crick Institute, London, England) with floxed histocompatibility 2, class II antigen A, beta 1 (IAB) mice (B6.129X1-H2-Ab1^{tm1Koni}/J, RRID:IMSR_JAX:013181; The Jackson Laboratory, Bar Harbor, ME). *Sox10^{CreERT2};IAB^{fl/fl}* animals are referred to here as glial^{MHC2KO}, and their *Sox10^{Cre};IAB^{fl/fl}* littermates as wild-type. RiboTag mice (*Rpl22^{tm1.1Psam}/J*) expressing hemagglutinin on ribosomal protein L22 (Rpl22; 011029; RRID:IMSR_JAX:011029; The Jackson Laboratory) were bred with the glial *Sox10^{CreERT2}* driver line to generate *Sox10^{CreERT2}/+;Rpl22^{tm1.1Psam}/J* mice.³⁷ *Sox10^{CreERT2}/+;Rpl22^{tm1.1Psam}/J* animals are referred to here as RiboTag animals. Enteric glial reporter mice (*Sox10^{CreERT2}/+;tdTomato*) were generated by breeding *Sox10^{CreERT2}/+* mice with Ai14 mice (B6.Cg-Gt(*ROSA*)26Sor^{tm14(CAG-tdTomato)Hze}/J; RRID:IMSR_JAX:007914; The Jackson Laboratory). CreERT2 activity was activated with a tamoxifen citrate diet (400 mg/kg) for 2 weeks.

Animal Sickness Severity Scoring

Animal sickness severity was scored as described previously.³⁸ Briefly, animals were scored from 0 to 4 on each of the following categories: appearance, level of consciousness, activity, response to stimulus, appearance of eyes, respiration rate, and respiration quality. Animals with a score greater than 21 or that lost >15% of their body weight were killed and were not included in the analysis.

Induction of Glial MHC-II

Mice were injected with IFN γ (1 μ g/mouse, intraperitoneally, cat. BMS326; eBioscience, Grand Island, NY), followed by intraperitoneal injection of *E coli* O111:B4 LPS (300 μ g/kg, cat. L4391; Millipore Sigma, St. Louis, MO) 2 hours afterward. Animal weights were measured at injection and before death. Animal sickness severity was scored as described previously.³⁸ Briefly, animals were scored from 0 to 4 on each of the following categories: appearance, level of consciousness, activity, response to stimulus, appearance of eyes, respiration rate, and respiration quality. Animals with a score greater than 21 or that lost >15% of their body weight were killed and not included in the analysis.

Phagocytosis Assay

Longitudinal muscle–myenteric plexus whole-mount preparations from glial reporter mice (*Sox10^{CreERT2}/+;tdTomato*) were incubated in Dulbecco's modified Eagle medium containing IFN γ (10 ng/mL, cat. BMS326; eBioscience), LPS (5 μ g/mL, cat. L4391; Millipore Sigma), and AlexaFluor-488–conjugated mouse anti-CD45.2 antibody (cat. 109816; BioLegend, San Diego, CA) and phagocytic substrates. Substrates were green pHrodo *E coli* BioParticles (1 mg/mL, cat. P35366; Thermo Fisher Scientific, Waltham, MA), AlexaFluor-488–labeled LPS (cat. L23351; Thermo Fisher Scientific) or FluoSpheres (1.0 μ m, cat. F8803; Thermo Fisher Scientific). Fluorescence was visualized by confocal, epifluorescence, and brightfield microscopy.

Whole-Mount Immunofluorescence

Colons were harvested, fecal pellets were flushed with phosphate-buffered saline (PBS), and tissues were fixed with Zamboni's fixative at 4°C overnight. Longitudinal muscle–myenteric plexus whole-mount preparations were processed via immunofluorescence as described previously.⁵ The antibodies and dilutions used are listed in Table 2. Labeled tissues were visualized by epifluorescence microscopy with a 40 \times objective (0.75 numeric aperture, Plan Fluor; Nikon, Melville, NY) on a Nikon Eclipse Ni upright microscope using a QImaging Retiga 2000R camera (Teledyne Photometrics, Tucson, AZ), or by confocal microscopy using an Olympus Fluoview FV1000 microscope (Olympus, Center Valley, PA) with a 60 \times Plan-Apochromat oil immersion objective (1.42 numeric aperture), achieving a resolution of 0.207 μ m/pixel in the X and Y image axis, and 0.4 μ m/slice in the Z axis. Immunofluorescence was

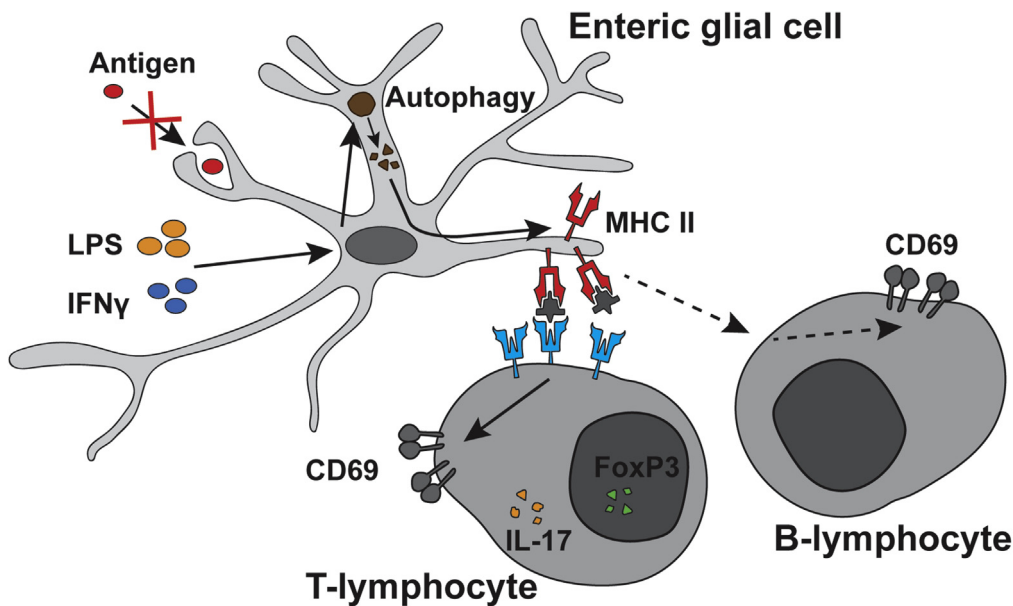


Figure 13. Schematic mechanism of enteric glial MHC-II expression. Enteric glia exposed to proinflammatory stimuli IFN γ and LPS up-regulate expression of MHC-II molecules on their cell surface. Enteric glial MHC-II is not derived from phagocytosed foreign antigens, but rather is derived from products of autophagy. Enteric glial MHC-II are functional molecules that can interact with B-lymphocytes, IL17-expressing, and FoxP3-expressing CD4 $^{+}$ T-lymphocytes to modulate CD69 expression.

quantified using Fiji software (<https://imagej.nih.gov/ij>, Bethesda, MD). Control experiments were performed by omitting primary antibodies in labeling protocols to control for nonspecific binding and autofluorescence.

H&E Staining

Colon tissues were fixed overnight in Zamboni's fixative at 4°C and washed with PBS. Tissues were embedded in paraffin and tissue sections (4- to 5- μ m thickness) were stained with H&E by the Michigan State University Investigative HistoPathology Laboratory.

Frozen Section Immunofluorescence

Mesenteric lymph nodes and spleens were fixed in Zamboni's fixative at 4°C overnight. Fixed samples were washed and incubated in a 30% sucrose solution in 0.1 mol/L phosphate buffer at 4°C for 72 hours. Samples were submitted to the Michigan State University HistoPathology Laboratory for cryosectioning, and 6- μ m-thick tissue sections were processed for immunolabeling as described earlier.

Flow Cytometry

Cells were isolated from mesenteric and inguinal lymph nodes and spleens by mechanical dissociation. Flow cytometric staining of cell surface and intracellular targets was performed as described previously³⁹ before analysis with a BD LSR II flow cytometer (Becton, Dickinson and Company, Franklin Lakes, NJ). Flow cytometry data were analyzed with FCS Express 7 Research Edition (De Novo Software, Pasadena, CA). Dead cells were identified and eliminated with the Zombie Yellow Fixable Viability Kit (cat. 423103; BioLegend), which was reconstituted as instructed and used as a 1:500 dilution in PBS for 15 minutes at room

temperature. Nonspecific binding of immunoglobulin to the fragment crystallizable (Fc) receptors was blocked by cell incubation with the TruStain FcX (anti-mouse CD16/32) antibody. Antibodies and dilutions are listed in Table 1. Doublets were eliminated by plotting forward scatter area vs height plot and gating for singlets. Unstained samples of mesenteric lymph node cells were used as controls to determine autofluorescence. UltraComp eBeads (Thermo Fisher Scientific) and the ArC Amine Reactive Compensation Bead Kit (for use with fixable dead cell stain kits, cat. A10346; Thermo Fisher Scientific) were used to calculate fluorescent compensation between each fluorophore. Fluorescence minus one controls were performed by labeling splenocytes or lymph node lymphocytes from LPS-stimulated littermate controls with all fluorophores except the one being measured.

Gene Expression

Sox10^{CreERT2 $^{+/-}$} ; *Rpl22*^{tm1.1Psam}/*J* mice were treated with a tamoxifen citrate diet (400 mg/kg) for 2 weeks to induce glial-specific ribosomal hemagglutinin-tag expression. Colons were harvested from RiboTag animals pretreated with IFN γ and then challenged with either LPS or saline (control), fecal pellets were flushed with PBS, and tissues were snap-frozen and stored at -80°C. Frozen tissues were homogenized using a GentleMACS Dissociator (Miltenyi Biotech, Auburn, CA) in M tubes running the program RNA_02, and RNA extraction and purification were performed as described previously.³⁷ Purified RNA was flash-frozen and submitted to the University of California Los Angeles Center for Systems Biomedicine core facility (Los Angeles, CA) for analysis via a custom NanoString nCounter multiplex panel. Gene expression levels were quantified based on counts of fluorescent barcodes specific to individual genes.

Cytokine Quantification

Serum samples collected at time of death were diluted 2-fold with PBS before quantification. Frozen colonic tissues were homogenized in a Tris-buffered saline Tween homogenization buffer using a GentleMACS Dissociator (Miltenyi Biotech) in M tubes running the program Protein_01. Cytokine/chemokine levels were quantified using a bead-based multiplex immunoassay (Eve Technologies, Calgary, Alberta, Canada).

Autophagy Induction and Detection

Live whole-mount preparations of myenteric plexus were prepared as described previously.⁵ Autophagy was induced with rapamycin (50 nmol/L, cat. 13346; Cayman Chemical, Ann Arbor, MI) or inhibited with 3-MA (5 mmol/L, cat.13242; Cayman Chemical) in Dulbecco's modified Eagle medium for 16 hours at 37°C. Autophagy was detected by measuring P62 immunofluorescence and LC3B puncta per cellular area. LC3B puncta was detected by thresholding the LC3B channel via the Intermodes algorithm in the Threshold function of Fiji, and quantified using the Analyze Particles function, setting particle size of interest from 0 to infinity, and circularity from 0 to 1.

Data Analysis

Confocal z-stack images were imported to Fiji software (version 1.53c; <https://imagej.nih.gov/ij>, National Institutes of Health, Bethesda, MD) using the Bio-Formats plugin (Open Microscopy Environment, University of Dundee, Dundee, UK). Measurements within glia were achieved by creating a mask around enteric glia using the Otsu algorithm in the Threshold function of Fiji. Measurements within enteric glia were achieved by subtracting glial measurements from a total ganglionic measurement. Mander's overlap coefficient was calculated with the Fiji plugin Just Another Colocalisation Plugin.⁴⁰ Line-scans across enteric ganglia in confocal z-stack images were performed using Metamorph software (Molecular Devices, San Jose, CA). Neuron density was assessed in myenteric plexus whole mounts labeled with GFAP and Hu antigens. To calculate neuronal density, the ganglionic area was estimated by using GFAP labeling to delineate the borders of enteric ganglia. Hu-labeled neurons within the estimated ganglionic area were counted manually, density was calculated, and the number of cells per ganglionic area was determined. Flow cytometric data were analyzed using FCS Express 7 Research Edition (De Novo Software) and gating cut-off values were determined using compensation and fluorescence minus one controls. We determined the activated fraction of each T-lymphocyte subtype by calculating the proportion of subtype marker and CD69 double-positive cells within the total number of subtype marker-positive cells. NanoString gene expression data were processed by nSolver v4.0 software (NanoString Technologies). Data are represented as fold change compared with the mean number of reads in saline control condition. For cytokine quantification, a 4-parameter logistic regression first was used to calculate the concentration of each analyte, and

samples below or above the logistic regression were designated as 0 or the highest standard curve value, respectively.

Statistics

All data are represented as means \pm SD and were analyzed by GraphPad Prism (versions 7 and 9.1.0; GraphPad Software, San Diego, CA). Immunofluorescence, flow cytometry, and quantified cytokine data were compared using unpaired 2-way ANOVA with Sidak- or Tukey-corrected multiple comparisons. $P < .05$ was set as the cut-off value for statistical significance. The Shapiro-Wilk test was used to check normality of data distributions. Outliers were detected in GraphPad Prism 7 using the ROUT method, with $Q = 1\%$ or 5% (1-sided 10% for Figure 4).

References

1. Dendrou CA, Petersen J, Rossjohn J, Fugger L. HLA variation and disease. *Nat Rev Immunol* 2018; 18:325–339.
2. Kambayashi T, Laufer TM. Atypical MHC class II-expressing antigen-presenting cells: can anything replace a dendritic cell? *Nat Rev Immunol* 2014; 14:719–730.
3. Jamwal DR, Laubitz D, Harrison CA, Figliuolo da Paz V, Cox CM, Wong R, Midura-Kiela M, Gurney MA, Besselsen DG, Setty P, Lybarger L, Bhattacharya D, Wilson JM, Ghishan FK, Kiela PR. Intestinal epithelial expression of MHCII determines severity of chemical, T-cell-induced, and infectious colitis in mice. *Gastroenterology* 2020;159:1342–1356.e6.
4. Kermarrec L, Durand T, Neunlist M, Naveilhan P, Neveu I. Enteric glial cells have specific immunosuppressive properties. *J Neuroimmunol* 2016;295–296:79–83.
5. Gulbransen BD, Sharkey KA. Purinergic neuron-to-glia signaling in the enteric nervous system. *Gastroenterology* 2009;136:1349–1358.
6. Barcelos Morais Da Silveira A, Oliveira EC De, Neto SG, Luquetti AO, Toshio Fujiwara R, Correa Oliveira R, Brehmer A, Barcelos A, Oliveira EC De, Neto SG, Luquetti AO, Toshio R, Correa R, Brehmer A. Enteroglia cells act as antigen-presenting cells in Chagasic megacolon. *Hum Pathol* 2011;42:522–532.
7. Turco F, Samelli G, Cirillo C, Palumbo I, Giorgi F De, D'Alessandro A, Cammarota M, Giuliano M, Cuomo R. Enteroglia-derived S100B protein integrates bacteria-induced Toll-like receptor signalling in human enteric glial cells. *Gut* 2014;63:105–115.
8. Geboes K, Rutgeerts P, Ectors N, Mebis J, Penninckx F, Vantrappen G, Desmet VJ. Major histocompatibility class II expression on the small intestinal nervous system in Crohn's disease. *Gastroenterology* 1992;103:439–447.
9. Rosenbaum C, Schick MA, Wollborn J, Heider A, Scholz C-J, Cecil A, Niesler B, Hirrlinger J, Walles H, Metzger M. Activation of myenteric glia during acute inflammation in vitro and in vivo. *PLoS One* 2016;11: e0151335.
10. Hyldig-Nielsen JJ, Schenning L, Hammerling U, Widmark E, Heldin E, Lind P, Serenius B, Lund T,

- Flavell R, Lee JS, Trowsdale J, Schreier PH, Zablitzky F, Larhammar D, Peterson PA, Rask L. The complete nucleotide sequence of the I-E alpha d immune response gene. *Nucleic Acids Res* 1983;11:5055–5071.
11. Mikkelsen HB. Macrophages in the external muscle layers of mammalian intestines. *Histol Histopathol* 1995; 10:719–736.
 12. Drokhyansky E, Smillie CS, Wittenberghe N Van, Ericsson M, Griffin GK, Eraslan G, Dionne D, Cuoco MS, Goder-Reiser MN, Sharova T, Kuksenko O, Aguirre AJ, Boland GM, Graham D, Rozenblatt-Rosen O, Xavier RJ, Regev A. The human and mouse enteric nervous system at single-cell resolution. *Cell* 2020;182:1606–1622.e23.
 13. Roche PA, Furuta K. The ins and outs of MHC class II-mediated antigen processing and presentation. *Nat Rev Immunol* 2015;15:203–216.
 14. Pabois J, Durand T, Berre C Le, Gonzales J, Neunlist M, Bourreille A, Naveilhan P, Neveu I. T cells show preferential adhesion to enteric neural cells in culture and are close to neural cells in the myenteric ganglia of Crohn's patients. *J Neuroimmunol* 2020;349:577422.
 15. Liñán-Rico A, Turco F, Ochoa-Cortes F, Harzman A, Needleman BJ, Arsenescu R, Abdel-Rasoul M, Fadda P, Grants I, Whitaker E, Cuomo R, Christofi FL. Molecular signaling and dysfunction of the human reactive enteric glial cell phenotype: implications for GI infection, IBD, POI, neurological, motility, and GI disorders. *Inflamm Bowel Dis* 2016;22:1812–1834.
 16. Wang D, Wu F, Yuan H, Wang A, Kang GJ, Truong T, Chen L, McCallion AS, Gong X, Li S. Sox10+ cells contribute to vascular development in multiple organs—brief report. *Arterioscler Thromb Vasc Biol* 2017; 37:1727–1731.
 17. Xia F, Deng C, Jiang Y, Qu Y, Deng J, Cai Z, Ding Y, Guo Z, Wang J. IL4 (interleukin 4) induces autophagy in B cells leading to exacerbated asthma. *Autophagy* 2018; 14:450–464.
 18. Mizushima N, Yoshimori T, Levine B. Methods in mammalian autophagy research. *Cell* 2010; 140:313–326.
 19. Dengjel J, Schoor O, Fischer R, Reich M, Kraus M, Müller M, Kreyborg K, Altenberend F, Brandenburg J, Kalbacher H, Brock R, Driessen C, Rammensee H, Stevanovic S. Autophagy promotes MHC class II presentation of peptides from intracellular source proteins. *Proc Natl Acad Sci U S A* 2005;102:7922–7927.
 20. Copeland S, Warren HS, Lowry SF, Calvano SE, Remick D. Acute inflammatory response to endotoxin in mice and humans. *Clin Diagn Lab Immunol* 2005; 12:60–67.
 21. Cheng S, Ma X, Geng S, Jiang X, Li Y, Hu L, Li J, Wang Y, Han X. Fecal microbiota transplantation beneficially regulates intestinal mucosal autophagy and alleviates gut barrier injury. *mSystems* 2018;3:e00137–18.
 22. Donohoe DR, Garge N, Zhang X, Sun W, O'Connell TM, Bunger MK, Bultman SJ. The microbiome and butyrate regulate energy metabolism and autophagy in the mammalian colon. *Cell Metab* 2011;13:517–526.
 23. Thelemann C, Eren RO, Coutaz M, Brasseit J, Bouzourene H, Rosa M, Duval A, Lavanchy C, Mack V, Mueller C, Reith W, Acha-Orbea H. Interferon- γ induces expression of MHC class II on intestinal epithelial cells and protects mice from colitis. *PLoS One* 2014;9:1–10.
 24. Ranasinghe S, Lamothe PA, Soghoian DZ, Kazer SW, Cole MB, Shalek AK, Yosef N, Jones RB, Donaghey F, Nwonu C, Jani P, Clayton GM, Crawford F, White J, Montoya A, Power K, Allen TM, Streeck H, Kaufmann DE, Picker LJ, Kappler JW, Walker BD. Antiviral CD8+ T cells restricted by human leukocyte antigen class II exist during natural HIV infection and exhibit clonal expansion. *Immunity* 2016;45:917–930.
 25. Lokensgard JR, Mutnal MB, Prasad S, Sheng W, Hu S. Glial cell activation, recruitment, and survival of B-lineage cells following MCMV brain infection. *J Neuroinflammation* 2016;13:1–15.
 26. Chaudhry A, Samstein RM, Treuting P, Liang Y, Pils MC, Heinrich J, Jack RS, Wunderlich FT, Brüning JC, Müller W, Rudensky AY. Interleukin-10 signaling in regulatory T cells is required for suppression of Th17 cell-mediated inflammation. *Immunity* 2011;34:566–578.
 27. McGeachy MJ, Bak-Jensen KS, Chen Y, Tato CM, Blumenschein W, McClanahan T, Cua DJ. TGF- β and IL-6 drive the production of IL-17 and IL-10 by T cells and restrain TH-17 cell-mediated pathology. *Nat Immunol* 2007;8:1390–1397.
 28. Wildenberg ME, Vos ACW, Wolfkamp SCS, Duijvestein M, Verhaar AP, Velde AA Te, Brink GR Van Den, Hommes DW. Autophagy attenuates the adaptive immune response by destabilizing the immunologic synapse. *Gastroenterology* 2012;142:1493–1503.e6.
 29. Brown IAM, McClain JL, Watson RE, Patel BA, Gulbransen BD. Enteric glia mediate neuron death in colitis through purinergic pathways that require connexin-43 and nitric oxide. *Cell Mol Gastroenterol Hepatol* 2016;2:77–91.
 30. Abdo H, Mahé MM, Derkinderen P, Bach-Ngohou K, Neunlist M, Lardeux B. The omega-6 fatty acid derivative 15-deoxy- $\Delta^{12,14}$ -prostaglandin J2 is involved in neuroprotection by enteric glial cells against oxidative stress. *J Physiol* 2012;590:2739–2750.
 31. Volchenkov R, Karlisen M, Jonsson R, Appel S. Type 1 regulatory T cells and regulatory B cells induced by tolerogenic dendritic cells. *Scand J Immunol* 2013; 77:246–254.
 32. Vilalta A, Brown GC. Neurophagy, the phagocytosis of live neurons and synapses by glia, contributes to brain development and disease. *FEBS J* 2018;285:3566–3575.
 33. Coelho-Aguiar J de M, Bon-Frauches AC, Gomes ALT, Verissimo CP, Aguiar DP, Matias D, Thomasi BB de M, Gomes AS, Brito GA de C, Moura-Neto V. The enteric glia: identity and functions. *Glia* 2015;63:921–935.
 34. Macias-Ceja DC, Cosín-Roger J, Ortiz-Masiá D, Salvador P, Hernández C, Esplugues JV, Calatayud S, Barrachina MD. Stimulation of autophagy prevents intestinal mucosal inflammation and ameliorates murine colitis. *Br J Pharmacol* 2017;174:2501–2511.
 35. Takeuchi H, Kondo Y, Fujiwara K, Kanzawa T, Aoki H, Mills GB, Kondo S. Synergistic augmentation of rapamycin-induced autophagy in malignant glioma cells

- by phosphatidylinositol 3-kinase/protein kinase B inhibitors. *Cancer Res* 2005;65:3336–3346.
36. Laranjeira C, Sandgren K, Kessar N, Richardson W, Potocnik A, Vanden Berghe P, Pachnis V. Glial cells in the mouse enteric nervous system can undergo neurogenesis in response to injury. *J Clin Invest* 2011; 121:3412–3424.
 37. Delvalle NM, Dharshika C, Morales-Soto W, Fried DE, Gaudette L, Gulbransen BD. Communication between enteric neurons, glia, and nociceptors underlies the effects of tachykinins on neuroinflammation. *Cell Mol Gastroenterol Hepatol* 2018;6:321–344.
 38. Shrum B, Anantha RV, Xu SX, Donnelly M, Haeryfar S, McCormick JK, Mele T. A robust scoring system to evaluate sepsis severity in an animal model. *BMC Res Notes* 2014;7:233.
 39. Maciorowski Z, Chattopadhyay PK, Jain P. Basic multi-color flow cytometry. *Curr Protoc Immunol* 2017;117:5.4.1–5.4.38.
 40. Bolte S, Cordelières FP. A guided tour into subcellular colocalization analysis in light microscopy. *J Microsc* 2006;224:213–232.

Received November 26, 2020. Accepted June 10, 2021.

Correspondence

Address correspondence to: Brian Gulbransen, PhD, Department of Physiology, Michigan State University, 567 Wilson Road, East Lansing, Michigan 48824. e-mail: gulbrans@msu.edu; fax: (517) 355-5125.

CRediT Authorship Contributions

Aaron K. Chow (Conceptualization: Equal; Data curation: Lead; Formal analysis: Lead; Investigation: Lead; Methodology: Equal; Validation: Equal; Visualization: Equal; Writing – original draft: Lead; Writing – review & editing: Equal)

Vladimir Grubišić, MD, PhD (Data curation: Supporting; Formal analysis: Supporting; Investigation: Supporting; Methodology: Supporting; Validation: Supporting; Visualization: Supporting; Writing – review & editing: Supporting)

Brian D. Gulbransen, PhD (Conceptualization: Equal; Data curation: Supporting; Formal analysis: Supporting; Funding acquisition: Lead; Investigation: Equal; Methodology: Equal; Project administration: Lead; Resources: Equal; Supervision: Lead; Validation: Equal; Visualization: Equal; Writing – original draft: Supporting; Writing – review & editing: Equal)

Conflicts of interest

The authors disclose no conflicts.

Funding

This work was supported by NIH National Institute of Diabetes and Digestive and Kidney grants R01DK103723 and R01DK120862 (B.D.G.), and Crohn's and Colitis Foundation Research Fellowship Award 577598 (V.G.).